J Physiol (2003), **550.3**, *pp.* 765–783

DOI: 10.1113/jphysiol.2003.040345
www.jphysiol.org

Journal of Physiology

Pyruvate modulates cardiac sarcoplasmic reticulum Ca^{2+} release in rats via mitochondria-dependent and -independent mechanisms

Aleksey V. Zima, Jens Kockskämper, Rafael Mejia-Alvarez and Lothar A. Blatter

Department of Physiology, Stritch School of Medicine, Loyola University Chicago, 2160 South First Avenue, Maywood, IL 60153, USA

The glycolytic product pyruvate has beneficial effects on cardiac contractile function. The postulated cellular mechanisms underlying the positive inotropic effect of pyruvate, however, are contradictory or have remained elusive. Therefore, we studied the effects of pyruvate on cardiac Ca^{2+} regulation, intracellular pH (pH_i) and flavoprotein oxidation using fluorescence confocal microscopy in intact and permeabilized rat ventricular myocytes and single channel recordings from rat cardiac ryanodine receptors (RyRs) incorporated into planar lipid bilayers. In intact cells extracellular pyruvate (10 mM) elevated diastolic $[Ca^{2+}]_i$, which was due, at least in part, to a concomitant acidification of the cytosol. Furthermore, pyruvate increased the amplitude and slowed the kinetics of the electrically evoked $[Ca^{2+}]_i$ transient, and augmented sarcoplasmic reticulum (SR) Ca^{2+} content. Recording of flavoprotein (FAD) fluorescence indicated that pyruvate caused a reduction of mitochondrial redox potential, which is proportional to an increase of the rate of ATP synthesis. Inhibitors of mitochondrial monocarboxylate transport (α-cyano-4-hydroxycinnamate, 0.5 mM), adenine nucleotide translocation (atractyloside, 0.3 mM) and the electron transport chain (cyanide, 4 mM) abolished or attenuated the pyruvate-mediated increase of the amplitude of the $[Ca^{2+}]_i$ transient, but did not change the effect of pyruvate on diastolic $[Ca^{2+}]_i$. Results from experiments with permeabilized myocytes indicated a direct correlation between ATP/ADP ratio and SR Ca^{2+} content. Furthermore, pyruvate (4 mM) reduced the frequency of spontaneous Ca^{2+} sparks by ~50 %. Single RyR channel recordings revealed a ~60 % reduction of the open probability of the channel by pyruvate (1 mM), but no change in conductance. This effect of pyruvate on RyR channel activity was neither Ca^{2+} nor ATP dependent. Taken together, these findings suggest that, in cardiac tissue, pyruvate has a dual effect on SR Ca^{2+} release consisting of a direct inhibition of RyR channel activity and elevation of SR Ca^{2+} content. The latter effect was most probably mediated by an enhanced SR Ca^{2+} uptake due to an augmentation of mitochondria-dependent ATP synthesis.

(Resubmitted 27 January 2003; accepted after revision 6 May 2003; first published online 24 June 2003)
Corresponding author L. A. Blatter: Department of Physiology, Stritch School of Medicine, Loyola University Chicago, 2160 South First Avenue, Maywood, IL 60153, USA. Email: lblatte@lumc.edu

In recent years tremendous efforts have been made to find novel inotropic drugs to enhance cardiac energetics and performance without jeopardizing the energy reserves of the injured heart. Evidence is emerging that pyruvate might be a promising, clinically useful positive inotropic agent fulfilling these conditions (Lopaschuk *et al.* 2002). Pyruvate, a product of glycolysis and substrate of the Krebs cycle, has been shown to improve mechanical performance of the heart under normoxic conditions (Zweier & Jacobus, 1987; Bünger *et al.* 1989; Mallet & Bünger, 1994; Yanos *et al.* 1994; Mallet & Sun, 1999) as well as during ischaemia–reperfusion injury (Bünger *et al.* 1989; Mallet *et al.* 1990; Zhou *et al.* 1995; for review see Mallet, 2000). Recent studies have even demonstrated that pyruvate is able to potentiate the positive inotropic effects of β-adrenergic stimulation (Hermann *et al.* 2000) and to improve the contractile performance of isolated failing human myocardium (Hasenfuss *et al.* 2002). In patients with heart failure, stimulation of pyruvate oxidation by either intracoronary application of pyruvate (Hermann *et al.* 1999) or intravenous administration of dichloroacetate (to increase mitochondrial pyruvate metabolism; Bersin *et al.* 1994) improved haemodynamics and myocardial function without the adverse effects of increased myocardial oxygen consumption observed under β-adrenergic stimulation (Bersin *et al.* 1994).

In spite of the emerging consent about the beneficial effects of pyruvate on cardiac performance, the cellular mechanisms of pyruvate action have remained unclear or even contradictory. There is, however, strong evidence that pyruvate improves the energetic conditions of cardiac

cells. With normal oxygen supply, pyruvate undergoes oxidation in the mitochondria, leading to augmentation of the NADH/NAD^+ reducing level and therefore to an increase of the driving force for ATP synthesis (Laughlin & Heineman, 1994; Scholz *et al.* 1995). Results from whole heart experiments indicate that the pyruvate inotropism is dependent on the mitochondrial metabolism of pyruvate (Mallet & Sun, 1999) and is associated with increases of the [phosphocreatine]/[inorganic phosphate] ($[P_i]$) ratio, ATP synthesis from phosphocreatine, and the cytosolic phosphorylation potential ([ATP]/([ADP][P_i])) (Zweier & Jacobus, 1987; Bünger *et al.* 1989; Mallet & Bünger, 1994). The cytosolic phosphorylation potential determines the free energy available from ATP hydrolysis, ΔG_{ATP}. Thus, an increase in phosphorylation potential would improve the efficiency of ATP-dependent processes, especially those participating in the contraction–relaxation cycle, such as the acto-myosin ATPase and the sarcoplasmic reticulum (SR) Ca^{2+}-ATPase. In the rabbit heart, a pyruvate-induced elevation of ΔG_{ATP} has been shown to increase the Ca^{2+} gradient between the SR and the cytosol, presumably due to increased SR Ca^{2+} pumping (Chen *et al.* 1998). Likewise, in the guinea-pig heart, pyruvate inotropism was mediated by an increased SR Ca^{2+} turnover as the result of elevated cytosolic energy levels (Mallet & Bünger, 1994; Mallet & Sun, 1999). Enhanced accumulation of Ca^{2+} by the SR is expected to increase Ca^{2+} release during each cardiac cycle and hence to augment the cytosolic $[Ca^{2+}]_i$ transient and contraction.

A different mode of inotropic action of pyruvate may involve changes in cytoplasmic pH (pH_i). The uptake of pyruvate into cardiac myocytes is mediated by a sarcolemmal H^+-monocarboxylate symporter (Poole & Halestrap, 1993). Thus, pyruvate uptake is expected to cause intracellular acidification, which, in turn, could affect contractility in multiple ways (for review see Bers, 2001). On the one hand, acidosis decreases the Ca^{2+} sensitivity of the contractile proteins (Fabiato & Fabiato, 1978) as well as the activity of the ryanodine receptor (RyR) Ca^{2+} release channel (Xu *et al.* 1996) and the SR Ca^{2+} ATPase (Fabiato & Fabiato, 1978; Mandel *et al.* 1982). On the other hand, these inhibitory effects of lowered pH_i could be compensated for by a higher SR Ca^{2+} load as a consequence of reduced SR Ca^{2+} release through RyRs (Hulme & Orchard, 1998; Balnave & Vaughan-Jones, 2000; Choi *et al.* 2000) and diminished Ca^{2+} extrusion through sarcolemmal Na^+–Ca^{2+} exchange (Bountra & Vaughan-Jones, 1989; Harrison *et al.* 1992). The situation becomes even more complex when the differing effects pyruvate can exert on pH_i itself are taken into account. It has been reported that in mammalian cardiac tissue pyruvate can cause sustained acidosis (de Hemptinne *et al.* 1983; Blatter & McGuigan, 1991) or transient acidification followed by sustained alkalinization (Hasenfuss *et al.* 2002).

Aside from the beneficial effects on cardiac performance, pyruvate may also exert pro-arrhythmogenic effects by causing cardiac alternans. Recent evidence from our laboratory suggests that pyruvate can elicit alternations of $[Ca^{2+}]_i$ transient amplitude, contraction strength, and action potential duration in both atrial and ventricular myocytes from the cat heart (Hüser *et al.* 2000; Kockskämper & Blatter, 2002; Blatter *et al.* 2003). Pyruvate-induced Ca^{2+} alternans was particularly pronounced in atrial myocytes. It exhibited large subcellular inhomogeneities and could generate arrhythmogenic Ca^{2+} waves. The suggested mode of pyruvate action involved feedback inhibition of glycolysis through stimulation of mitochondrial metabolism although direct experimental evidence for this hypothesis is lacking.

In summary, previous studies on the effects of pyruvate on cardiac performance have revealed both salutary and adverse actions. Systematic investigations into the underlying mechanisms of pyruvate action are sparse and have yielded controversial results. Therefore, we undertook a detailed study on the effects of pyruvate on mitochondrial redox state and energy metabolism, and on Ca^{2+} and H^+ homeostasis in rat ventricular myocytes. Part of this work has been published in abstract form (Zima *et al.* 2002).

METHODS

Isolation of rat ventricular myocytes

Rat ventricular myocytes were enzymatically isolated as described previously (Bers *et al.* 1990). The procedure for cell isolation was approved by the Institutional Animal Care and Use Committee of Loyola University Chicago, Stritch School of Medicine. Briefly, rats were anaesthetized by intraperitoneal injection of sodium pentobarbital (100 mg kg^{-1}). Hearts were removed quickly and flushed with nominally Ca^{2+}-free Tyrode solution containing (mM): NaCl 140; KCl 4; $MgCl_2$ 1; glucose 10; and Hepes 10; pH 7.4 (NaOH). Hearts were mounted on a Langendorff apparatus and perfused with Ca^{2+}-free Tyrode solution for 5 min at 37 °C. Perfusion was then switched to Ca^{2+}-free Tyrode solution containing 1 mg ml^{-1} collagenase (type I, Sigma) and 0.16 mg ml^{-1} protease (type XIV, Sigma) for 7 min. Subsequently hearts were washed with 50 ml Ca^{2+}-free Tyrode solution. The digested ventricular tissue was minced, triturated and filtered. Isolated cells were resuspended in normal Tyrode solution (1 mM $CaCl_2$) and kept at room temperature (22–24 °C) until used for experimentation.

Measurement of $[Ca^{2+}]_i$ transients in intact cells

Myocytes were loaded with the Ca^{2+} indicator fluo-4 by 20 min incubation in Tyrode solution containing 20 μM fluo-4 AM (fluo-4 acetoxymethyl ester; Molecular Probes, Eugene, OR, USA) at room temperature. A glass coverslip with the cells was mounted in an experimental chamber on the stage of an inverted microscope (Nikon Eclipse TE300). Cells were superfused continuously with normal Tyrode solution (1 ml min^{-1}). A period of 15–20 min was allowed for de-esterification of the dye. Experiments were carried out at room temperature (22–24 °C).

$[Ca^{2+}]_i$ measurements in isolated rat ventricular myocytes were performed using a laser scanning confocal microscope (Radiance 2000 MP, Bio-Rad, UK) equipped with a × 40 oil-immersion

objective lens (NA = 1.3). Fluo-4 was excited with the 488 nm line of an argon ion laser and fluorescence was measured at wavelengths > 515 nm. Images were acquired in the linescan mode (3 or 6 ms $scan^{-1}$; pixel size 0.3 μm). The scan line was oriented parallel to the longitudinal axis of the cell avoiding the nucleus. Whole-cell $[Ca^{2+}]_i$ transients were obtained by averaging the entire cellular fluo-4 signal from the scanned line. $[Ca^{2+}]_i$ transients are presented as background-subtracted normalized fluorescence (F/F_0) where F is the fluorescence intensity and F_0 is resting fluorescence recorded under steady-state conditions at the beginning of an experiment. $[Ca^{2+}]_i$ transients were evoked by electrical field stimulation with 2 ms suprathreshold voltage pulses applied through a pair of extracellular platinum electrodes at a frequency of 0.5 Hz.

Measurement of Ca^{2+} sparks in permeabilized cells

Ventricular myocytes were permeabilized with saponin (Endo & Kitazawa, 1978; Lukyanenko & Györke, 1999). First, the cells were suspended in a solution containing (mM): potassium aspartate 100; KCl 20; EGTA 0.5; $MgCl_2$ 0.75; and Hepes 10; pH 7.2 (KOH), and placed in the experimental chamber (final volume 50 μl) for 15 min. The cell surface membrane was permeabilized by adding 0.005 % (w/v) saponin for 30 s. After 30 s the bath solution was exchanged to a saponin-free internal solution composed of (mM): potassium aspartate 100; KCl 15; KH_2PO_4 5; MgATP 5; EGTA 0.5; $CaCl_2$ 0.12; $MgCl_2$ 0.75; phosphocreatine 10; Hepes 10; and fluo-3 potassium salt 0.03; with creatine phosphokinase 5 U ml^{-1}; dextran (MW: 40 000) 8 %; pH 7.2 (KOH). Free $[Ca^{2+}]$ and $[Mg^{2+}]$ of this solution were 100 nM and 1 mM, respectively (calculated using WinMAXC 2.05, Stanford University, CA, USA). In the experiments studying the effects of the [ATP]/[ADP] ratio on SR Ca^{2+} release, phosphocreatine and creatine phosphokinase were omitted from the internal solution. During experiments, the solutions were changed by simple replacement. Ca^{2+} sparks were recorded in the linescan mode of the laser scanning confocal system as described above. Ca^{2+} sparks were detected and quantified in terms of amplitude and frequency using an automated detection algorithm (Cheng *et al.* 1999). Ca^{2+} spark frequencies are expressed as the number of observed sparks per second and per 100 μm of scanned distance in the confocal linescan mode (sparks s^{-1} (100 $\mu m)^{-1}$).

pH measurements in intact cells

Intracellular pH (pH_i) was measured using laser scanning confocal microscopy. Cells were loaded with the pH indicator 5-(and 6-)carboxy SNARF-1 (Molecular Probes) by 30–40 min exposure to Tyrode solution containing 9 μM of the membrane-permeant form (acetoxymethylester acetate) of the dye. For ratiometric pH imaging, carboxy SNARF-1 was excited with the 514 nm line of the argon ion laser, and emitted fluorescence was collected simultaneously at 590 ± 35 nm (F_{590}) and at > 650 nm ($F_{>650}$). Relative changes of intracellular pH are expressed as changes of the ratio $R = F_{>650}/F_{590}$, with higher values of R indicating alkalinization and lower values indicating acidification. To minimize photobleaching and cell damage, two-dimensional images (pixel size: 0.25–0.34 μm) of the myocytes were acquired at 15 s intervals.

Measurement of flavoprotein (FAD) fluorescence in intact cells

The mitochondrial redox state of single myocytes was assessed by measuring flavin adenine dinucleotide (FAD)-linked protein fluorescence using laser scanning confocal microscopy (Romashko *et al.* 1998). Endogenous FAD autofluorescence was excited at 488 nm with an argon ion laser and fluorescence was measured at wavelengths > 515 nm. Two-dimensional images were acquired at 15 s intervals. The relative changes in FAD fluorescence are presented as background-subtracted normalized fluorescence (F/F_0) where F is the fluorescence intensity and F_0 is the initial fluorescence recorded under steady-state conditions at the beginning of an experiment. Fluorescence intensity was integrated over regions of interest (10 μm × 10 μm) excluding the nuclei and the edges of the cell.

SR microsome preparation

SR microsomes were obtained from rat ventricles. Rats were anaesthetized with intraperitoneal injection of sodium pentobarbital (100 mg kg^{-1}). Hearts were quickly removed by thoracotomy and rinsed in Ca^{2+}-free Tyrode solution. After atrial and vascular tissues (aorta and pulmonary artery remains) were trimmed off, the ventricles were blotted on filter paper to remove excess solution. The ventricles were homogenized in cold saline solution of the following composition (mM): NaCl 154; and Trizma-maleate 10; pH 6.8. The homogenate was spun at 7000 r.p.m. (4000 *g*) for 20 min and the pellet discarded. This supernatant was spun at 10 000 r.p.m. (8000 *g*) for 20 min, and the resulting supernatant was spun in the ultracentrifuge at 47 000 r.p.m. (100 000 *g*) for 40 min. The final pellet was resuspended in storage solution (mM): NaCl 154; Trizma-maleate 10; and sucrose 300; pH 6.8; then flash frozen and stored at −80 °C until used. The whole procedure was carried out in a cold room, at 4 °C and in the presence of protease inhibitors (μM: aprotinin 0.1, benzamidine 500, leupeptine 1, pepstatin A 1 and phenylmethylsulphonyl fluoride (PMSF) 200).

Ryanodine receptor single channel recordings

Planar lipid bilayers were formed from a lipid mixture containing phosphatidylethanolamine, phosphatidylserine and phosphatidylcholine (ratio 5:4:1) dissolved in *n*-decane at a final lipid concentration of 45 mg ml^{-1}. SR vesicles were added to the *cis*-chamber, which corresponded to the cytosolic side of the RyR channel. The *trans*-chamber (lumenal side of RyR) was connected to the virtual ground of the amplifier. During fusion, the *cis*- and *trans*-chambers contained solutions of the following composition (mM): $CsCH_3SO_3$ 400 (*cis*) and 40 (*trans*), respectively; $CaCl_2$ 0.1; Hepes 20; pH 7.3 (CsOH). After channel incorporation, the concentration of $CsCH_3SO_3$ in the *trans*-chamber was increased to 400 mM and free $[Ca^{2+}]$ in the *cis*-chamber was adjusted to various levels (0.6–10 μM) by addition of EGTA. Free $[Ca^{2+}]$ in the experimental solutions was verified with a Ca^{2+}-sensitive mini-electrode (Baudet *et al.* 1994). Single-channel currents were recorded using an Axopatch 200B amplifier (Axon Instruments, Foster City, CA, USA). All recordings were made at a holding potential of −20 mV. Currents were filtered at 1 kHz and digitized at 5 kHz.

Drugs

Pyruvate (sodium salt), α-cyano-4-hydroxycinnamate (CIN), atractyloside (ATR), carbonyl *p*-trifluoromethoxy-phenylhydrazone (FCCP), oligomycin and ryanodine were obtained from Sigma (St Louis, MO, USA). Cariporide was a gift from Aventis Pharma Deutschland GmbH. In normal Tyrode solution containing sodium pyruvate, NaCl was reduced by equimolar amounts to keep $[Na^+]$ constant. CIN was dissolved in methanol before being added to the experimental solution. ATR, oligomycin, FCCP and ryanodine were dissolved in ethanol. The final concentration of solvent in the experimental solutions was less then 0.1 % which had no apparent effect on $[Ca^{2+}]_i$.

Data analysis

Data are presented as means ± S.E.M. of n cells or RyR bilayers. Statistical comparisons between groups were performed with Student's t test. Differences were considered statistically significant at $P < 0.05$.

RESULTS

Pyruvate increases resting $[Ca^{2+}]_i$ and the systolic $[Ca^{2+}]_i$ transient

Figure 1*A* shows the effects of 10 mM pyruvate on action potential-induced whole-cell $[Ca^{2+}]_i$ transients obtained from confocal linescan images of a fluo-4-loaded rat ventricular myocyte. $[Ca^{2+}]_i$ transients were evoked by electrical field stimulation at a frequency of 0.5 Hz. The application of pyruvate (horizontal bar above the traces) increased both diastolic and peak systolic $[Ca^{2+}]_i$, as well as the $[Ca^{2+}]_i$ transient amplitude defined as the difference between peak systolic $[Ca^{2+}]_i$ and diastolic $[Ca^{2+}]_i$. Both effects were largely reversible (Fig. 1*A* and *B*).

Figure 1*B* presents average data for the effect of pyruvate on diastolic $[Ca^{2+}]_i$ and $[Ca^{2+}]_i$ transient amplitude. Both diastolic $[Ca^{2+}]_i$ and $[Ca^{2+}]_i$ transient amplitude were normalized to the levels recorded at the beginning of the experiment (0′ in Fig. 1*A*). After 8 min of pyruvate application diastolic $[Ca^{2+}]_i$ increased by 57 ± 5 % ($n = 18$; $P < 0.001$) and $[Ca^{2+}]_i$ transient amplitude by 54 ± 11 % ($n = 18$; $P < 0.001$). The time courses of the respective changes, however, were markedly different. The increase of diastolic $[Ca^{2+}]_i$ occurred rapidly, reaching a new steady state after less than 4 min of pyruvate exposure. In contrast, the increase in $[Ca^{2+}]_i$ transient amplitude did not, on average, start until 1 min after the beginning of pyruvate exposure and took about 8 min to develop fully. In many cases (13 out of 24 cells) pyruvate initially caused a modest reduction of the $[Ca^{2+}]_i$ transient amplitude during the first minute. The mean value of the $[Ca^{2+}]_i$ transient amplitude after 1 min of pyruvate exposure, however, was not statistically different from control (3.1 ± 0.3 *vs.* 3.4 ± 0.2, $n = 24$).

Pyruvate also altered the kinetics of the $[Ca^{2+}]_i$ transient. Figure 1*C* shows normalized $[Ca^{2+}]_i$ transients on an expanded time scale. The $[Ca^{2+}]_i$ transients (marked by the arrows in Fig. 1*A*) were recorded under control conditions and after 8 min of pyruvate exposure. Pyruvate slowed the time-to-peak by 126 % from 64 ± 8 ms to 145 ± 17 ms ($n = 18$; $P < 0.002$). The declining phase of the $[Ca^{2+}]_i$ transient was fitted with a monoexponential function. Pyruvate tended to accelerate the decay, but overall had no significant effect on the time constant of decay (τ_{decay}; derived from the monoexponential fit) of the $[Ca^{2+}]_i$

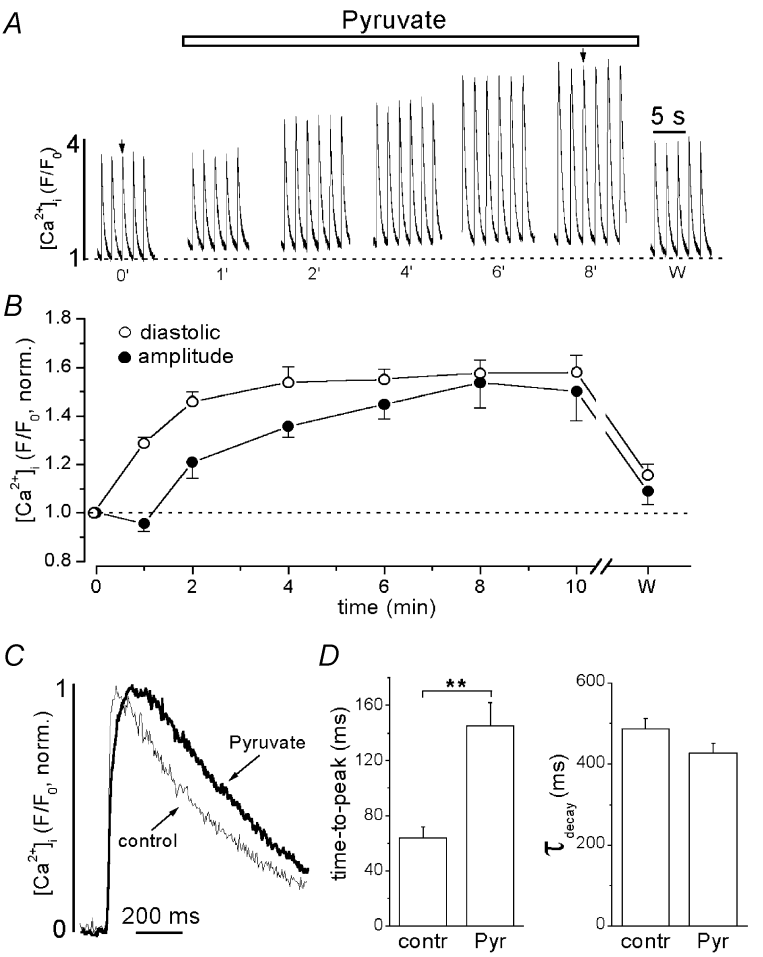

Figure 1. Effects of pyruvate on electrically evoked $[Ca^{2+}]_i$ transients in intact rat ventricular myocytes

A, action potential-induced $[Ca^{2+}]_i$ transients recorded under control conditions (0′), at different times during exposure to 10 mM pyruvate (as indicated by the numbers under the traces, in min), and after washout of pyruvate (w; recorded 4 min after removal of pyruvate). Stimulation frequency was 0.5 Hz. *B*, average data of pyruvate-mediated changes of diastolic $[Ca^{2+}]_i$ (○) and $[Ca^{2+}]_i$ transient amplitude (●). Values were normalized to the levels observed under control conditions (0′ in *A*). *C*, representative $[Ca^{2+}]_i$ transients were normalized, superimposed and displayed on an expanded time scale. The $[Ca^{2+}]_i$ transients were recorded under control conditions (thin line) and in the presence of pyruvate (thick line) at the times indicated by the arrows in *A*. *D*, summarized data of the effect of pyruvate on rise time of the $[Ca^{2+}]_i$ transient (time-to-peak was measured from 25 % above diastolic $[Ca^{2+}]_i$ to the peak of the $[Ca^{2+}]_i$ transient) and time constant of decline of $[Ca^{2+}]_i$ (τ_{decay}). ** Statistically different at $P < 0.002$.

transient (487 ± 26 ms in control conditions *vs.* 428 ± 24 ms in the presence of 10 mM pyruvate; $n = 18$; difference statistically not significant). The effects of pyruvate on the kinetics of $[Ca^{2+}]_i$ transients are summarized in Fig. 1*D*.

The observation that pyruvate increased diastolic $[Ca^{2+}]_i$ and the amplitude of the systolic $[Ca^{2+}]_i$ transient and, in addition, that it prolonged the rise time of the $[Ca^{2+}]_i$ transient suggested that the glycolytic product pyruvate exerted complex effects on cellular Ca^{2+} handling. The following experiments were designed to elucidate the underlying cellular mechanisms.

Pyruvate increases SR Ca^{2+} load

The amount of Ca^{2+} released by rapid caffeine application (10 mM) was used as an index of SR Ca^{2+} load. Figure 2 shows a representative experiment in which 10 mM caffeine was applied to an intact myocyte under control conditions, after 8 min of pyruvate (10 mM) exposure and after washout of pyruvate. Caffeine was applied for 3 s, 5 s after the last electrically evoked $[Ca^{2+}]_i$ transient. Clearly, pyruvate caused a significant increase in the amplitude of the caffeine-induced $[Ca^{2+}]_i$ elevation. On average, the amplitude of the caffeine response in the presence of pyruvate was 28 ± 6 % larger than under control conditions ($n = 6$; $P < 0.002$). This effect on SR Ca^{2+} content was completely reversible after washout of pyruvate. Hence, the effects of pyruvate on the $[Ca^{2+}]_i$ transient amplitude could, in part, be explained by an increase in SR Ca^{2+} load.

Involvement of pH in the effects of pyruvate on $[Ca^{2+}]_i$ transients

In cardiac tissue pyruvate uptake is mediated by a sarcolemmal H^+-monocarboxylate symporter. Thus, pyruvate uptake is expected to lead to intracellular acidification, although previous studies have yielded somewhat conflicting results (see Introduction). Therefore, the next experiments were designed to define the role of changes of intracellular pH (pH_i) for the pyruvate effects on $[Ca^{2+}]_i$.

For this purpose, we compared the effects of pyruvate (10 mM) and D-lactate (10 mM) on pH_i and $[Ca^{2+}]_i$. Pyruvate and D-lactate enter the cytoplasm by the same mechanisms (Poole & Halestrap, 1993) and, consequently, should affect pH_i in a similar fashion. Intracellular pH was measured directly in intact cells with the fluorescent indicator carboxy SNARF-1. Figure 3*A* shows the changes of pH_i resulting from the application of D-lactate and pyruvate to the same cell. Both compounds caused a rapid decrease of pH_i, which reached a new steady-state within about 1 min. The acidification during D-lactate or pyruvate exposure was sustained and readily reversible upon washout. Average pH_i changes induced by D-lactate and pyruvate are summarized in Fig. 3*Ca*. Data were normalized to pH_i levels recorded at the beginning of the experiment. On average pH_i (expressed as $R = F_{>650}/F_{590}$) decreased by 20 ± 2 % during exposure to D-lactate and by 18 ± 2 % ($n = 12$) during superfusion with pyruvate. The effects of D-lactate and pyruvate on pH_i were not statistically different from each other.

Since exposure to D-lactate and pyruvate generated the same degree of acidification, this protocol allowed us to distinguish between pH-dependent and pH-independent effects of pyruvate on $[Ca^{2+}]_i$. Figure 3*B* compares the effects of D-lactate and pyruvate exposure on $[Ca^{2+}]_i$ transients in rat ventricular myocytes. The diastolic $[Ca^{2+}]_i$ increased by 32 ± 4 % ($n = 6$) and 30 ± 2 % ($n = 24$) after D-lactate and pyruvate application, respectively, measured after 1 min, and by 41 ± 4 % ($n = 6$) and 55 ± 4 % ($n = 20$), respectively, after 6 min. The effects of D-lactate and

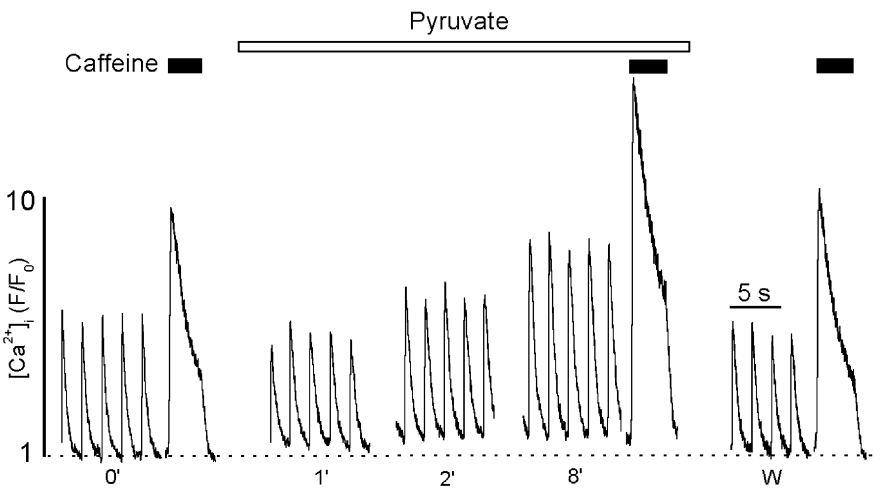

Figure 2. The effect of pyruvate on caffeine-induced Ca^{2+} release

$[Ca^{2+}]_i$ transients elicited by field stimulation and rapid application of 10 mM caffeine under control conditions (0′), during pyruvate treatment (time in min), and after washout of pyruvate (w; recorded 4 min after removal of pyruvate). In each case caffeine was applied 5 s after the last $[Ca^{2+}]_i$ transient for 3 s.

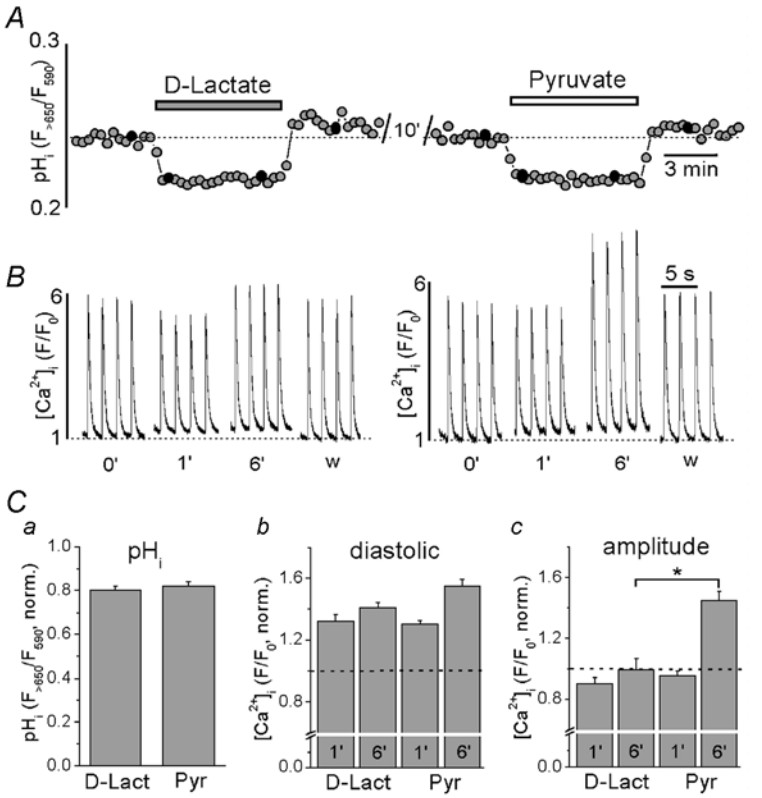

Figure 3. The effects of D-lactate and pyruvate on pH_i and $[Ca^{2+}]_i$ transients

A, changes of pH_i evoked by application of 10 mM D-lactate and 10 mM pyruvate recorded from a single ventricular myocyte. Relative changes in pH_i are expressed as changes in the carboxy SNARF-1 ratio signal ($R = F_{>650}/F_{590}$) where a decrease in R corresponds to a decrease in pH_i. *B*, effects of application of 10 mM D-lactate and pyruvate on action potential-induced $[Ca^{2+}]_i$ transients. The transients were recorded at the times indicated by black circles in *A* (time in min). pH_i and $[Ca^{2+}]_i$ were measured in different cells. *C*, summarized data of relative changes of pH_i (*a*), diastolic $[Ca^{2+}]_i$ (*b*) and $[Ca^{2+}]_i$ transient amplitudes (*c*) during the application of D-lactate and pyruvate. Numbers indicate time in minutes after application of D-lactate and pyruvate, respectively. Data were normalized to pH_i and $[Ca^{2+}]_i$ levels recorded at the beginning of the experiment. * Statistically different at $P < 0.05$.

pyruvate on diastolic $[Ca^{2+}]_i$ were not significantly different (Fig. 3*Cb*). Pyruvate and D-lactate, however, had different effects on the $[Ca^{2+}]_i$ transient amplitude (Fig. 3*Cc*). After 1 min, D-lactate slightly decreased the amplitude by 10 ± 4 % ($n = 6$), whereas pyruvate did not have any significant effect (there was a decrease of 4 ± 3 %; $n = 24$). After 6 min of D-lactate application, the $[Ca^{2+}]_i$ transient amplitude recovered to the control level (−1 ± 7 %, $n = 6$). In contrast, after the same time of exposure to pyruvate the $[Ca^{2+}]_i$ transient amplitude had increased by 45 ± 6 % ($n = 20$, $P < 0.001$ *vs.* control). The differences in $[Ca^{2+}]_i$ transient amplitude induced by D-lactate and pyruvate were statistically significant at the 6 min mark ($P < 0.05$). The effects of acidification produced by D-lactate on the kinetics of the $[Ca^{2+}]_i$ transient were small and not statistically significant. The time-to-peak and τ_{decay} were 70 ± 9 and 424 ± 27 ms, respectively ($n = 6$; statistically not different from control). Thus, the slowing of the rising phase of the $[Ca^{2+}]_i$ transient observed in the presence of pyruvate (Fig. 1*C*) appeared to be independent of intracellular acidosis.

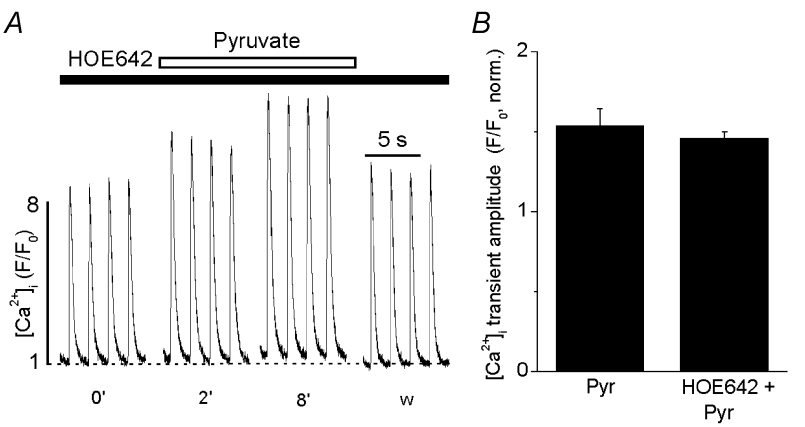

Figure 4. The effects of pyruvate on $[Ca^{2+}]_i$ transients during inhibition of Na^+–H^+ exchange

A, $[Ca^{2+}]_i$ transients were elicited by electrical field stimulation (time in min). Before exposure to pyruvate (10 mM) the cell was preincubated with cariporide (HOE642; 1 μM) to inhibit Na^+–H^+ exchange (NHE). *B*, average relative increase of $[Ca^{2+}]_i$ transient amplitude by pyruvate in the presence and absence of cariporide. $[Ca^{2+}]_i$ transient amplitudes were normalized to the amplitude measured at time 0´.

Cytosolic acidification results in an increase of $[Na^+]_i$ due to the compensatory removal of protons via the sarcolemmal Na^+–H^+ exchange (NHE) mechanism. This, in turn, may lead to enhanced SR Ca^{2+} load because of reduced Ca^{2+} extrusion via Na^+–Ca^{2+} exchange (see Introduction). To explore this possibility we measured the effect of pyruvate on $[Ca^{2+}]_i$ transients in the presence of the selective NHE inhibitor cariporide (HOE642; for review see Ravens & Himmel, 1999). In the presence of cariporide, pyruvate caused a gradual and reversible increase of the $[Ca^{2+}]_i$ transient amplitude (Fig. 4*A*). On average (Fig. 4*B*), in the presence of cariporide, pyruvate caused an increase of the $[Ca^{2+}]_i$ transient amplitude by $46 \pm 4\%$ ($n = 5$), which was not different from control ($54 \pm 11\%$; $n = 18$). The data indicate that a potential increase of $[Na^+]_i$ due to cytoplasmic acidification was not sufficient to explain the positive inotropic effect of pyruvate on the $[Ca^{2+}]_i$ transient amplitude.

In summary, D-lactate and pyruvate evoked similar degrees of intracellular acidification and elevation of diastolic $[Ca^{2+}]_i$, suggesting that the two phenomena are causally related. A change in pH_i, however, fails to explain the distinctly different effects on $[Ca^{2+}]_i$ transient amplitude, indicating that the pyruvate-mediated augmentation of the $[Ca^{2+}]_i$ transient and the slowing of its kinetics are mediated by other mechanisms.

Pyruvate decreases cellular FAD autofluorescence

To further explore the mechanism of pyruvate action our focus shifted towards the role of the mitochondria. There is evidence (see Introduction) that enhancement of cardiac contraction by pyruvate is directly associated with an increase of the cytosolic phosphorylation potential due to mitochondrial pyruvate oxidation. Thus, we investigated the possible link between pyruvate and the mitochondrial metabolic state. Respiratory ATP synthesis is highly dependent on the redox potential of the mitochondria (Laughlin & Heineman, 1994; Scholz *et al.* 1995). In the mitochondrial matrix, there is an equilibrium between the redox potential of the NADH/NAD^+ and the $FADH_2$/FAD pool (Vuorinen *et al.* 1995). Hence, principally either FAD-linked or NADH-linked autofluorescence can be used as a measure for the metabolic state of the mitochondria. In contrast to NADH fluorescence, however, which originates from both the cytosol and the mitochondria, FAD fluorescence originates exclusively from the mitochondria (Hassinen & Chance, 1968). Furthermore, pyruvate might alter cytosolic NADH levels through the lactate dehydrogenase reaction. Therefore, we chose to measure changes of the mitochondrial redox state by means of FAD rather than NADH fluorescence. Figure 5*A* shows that 10 mM pyruvate reversibly decreased FAD fluorescence (F/F_0) to 0.92 ± 0.02 ($n = 10$, $P < 0.05$), whereas 10 mM D-lactate had no significant effect (1.01 ± 0.02, $n = 6$, $P > 0.05$). The FAD signal decreased to a minimum in the presence of the cytochrome oxidase inhibitor cyanide (CN^-, 4 mM) and increased upon exposure to the mitochondrial uncoupler FCCP (1 μM). CN^- and FCCP are expected to cause maximum reduction and oxidation, respectively, of the flavoproteins. The average data for FAD fluorescence changes induced by pyruvate, D-lactate, CN^- and FCCP are summarized in Fig. 5*B*. Exposure to

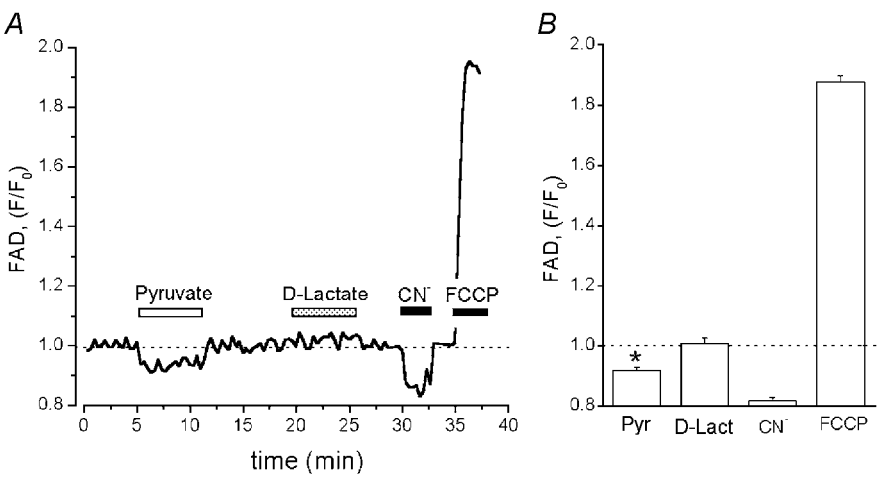

Figure 5. Effects of pyruvate and D-lactate on flavoprotein (FAD) autofluorescence

A, recording of FAD autofluorescence from a single ventricular myocyte. Pyruvate (10 mM), D-lactate (10 mM), CN^- (4 mM) and FCCP (1 μM) were added as indicated by horizontal bars above the trace. Downward deflection in FAD fluorescence trace denotes reduction. FAD fluorescence levels during exposure to CN^- and FCCP indicate maximum levels of reduction and oxidation, respectively. During FAD measurements the cells were electrically stimulated at a frequency of 0.5 Hz. *B*, summarized data of relative changes of FAD fluorescence during the application of pyruvate, D-lactate, CN^- and FCCP. Data were normalized to the FAD signal recorded at the beginning of the experiment. * Statistically different at $P < 0.05$ *vs.* control.

CN^- diminished the relative FAD fluorescence (F/F_0) to 0.82 ± 0.01 (n = 10), whereas during exposure to FCCP it increased to 1.88 ± 0.02 (n = 10). These results indicate that pyruvate induced a reduction of mitochondrial FAD fluorescence by 44 % relative to the effect of CN^- (maximum reduction level). Thus, we conclude that pyruvate increases the mitochondrial redox potential and, thereby, facilitates respiratory ATP synthesis.

Role of the mitochondria in the effects of pyruvate on the $[Ca^{2+}]_i$ transient

To further define the role of the mitochondria in the effects of pyruvate on $[Ca^{2+}]_i$ transients, inhibitors of mitochondrial monocarboxylate transport (α-cyano-4-hydroxycinnamate), the adenine nucleotide translocation mechanism (atractyloside) and the mitochondrial respiratory chain (CN^-) were used.

Inhibition of mitochondrial monocarboxylate transport. α-Cyano-4-hydroxycinnamate (CIN) in submillimolar concentrations selectively and reversibly inhibits mitochondrial pyruvate uptake (Bünger & Mallet, 1993). Pretreatment of rat ventricular myocytes with 0.5 mM CIN for 5 min resulted in a 23 ± 3 % reduction of the $[Ca^{2+}]_i$ transient amplitude from 3.5 ± 0.4 to 2.8 ± 0.3 (n = 7; P < 0.001). In contrast, CIN did not change diastolic $[Ca^{2+}]_i$ significantly. Figure 6*A* and *B* illustrates the effects of 10 mM pyruvate on $[Ca^{2+}]_i$ transients in the presence of 0.5 mM CIN. Figure 6*A* presents original $[Ca^{2+}]_i$ transients from a rat ventricular myocyte, whereas Fig. 6*B* shows average data normalized to control in the presence of CIN. Pretreatment with CIN completely abolished the stimulatory effect of pyruvate on the $[Ca^{2+}]_i$ transient amplitude. When pyruvate was added to the superfusion solution the $[Ca^{2+}]_i$ transient amplitude initially even decreased by 19 ± 1 % relative to the level in the presence of CIN alone (from 2.8 ± 0.3 to 2.3 ± 0.2; n = 7; P < 0.001). This inhibitory effect diminished during prolonged exposure to pyruvate, eventually reaching initial levels over the course of 6–8 min. Inhibition of mitochondrial pyruvate uptake by CIN, however, did not prevent the effects of pyruvate on diastolic $[Ca^{2+}]_i$. In the presence of CIN, pyruvate increased diastolic $[Ca^{2+}]_i$ by 46 ± 10 % (n = 7), which was not statistically different from the increase observed under control conditions (57 ± 5 %, Fig. 1*B*). Furthermore, the previously observed slowing down of the rising phase of the $[Ca^{2+}]_i$ transient by pyruvate (126 % increase in time-to-peak, Fig. 1*D*) was similar. With CIN present (Fig. 6*C*) pyruvate increased the time-to-peak by 105 % from 76 ± 10 ms to 160 ± 17 ms (n = 7; P < 0.002).

Inhibition of mitochondrial adenine nucleotide translocation. ATP is synthesized in the mitochondrial matrix and transferred to the cytosol by the mitochondrial adenine nucleotide translocator situated in the inner mitochondrial membrane. To determine whether enhanced mitochondrial ATP synthesis was involved in the pyruvate-mediated augmentation of the $[Ca^{2+}]_i$ transient, the effect

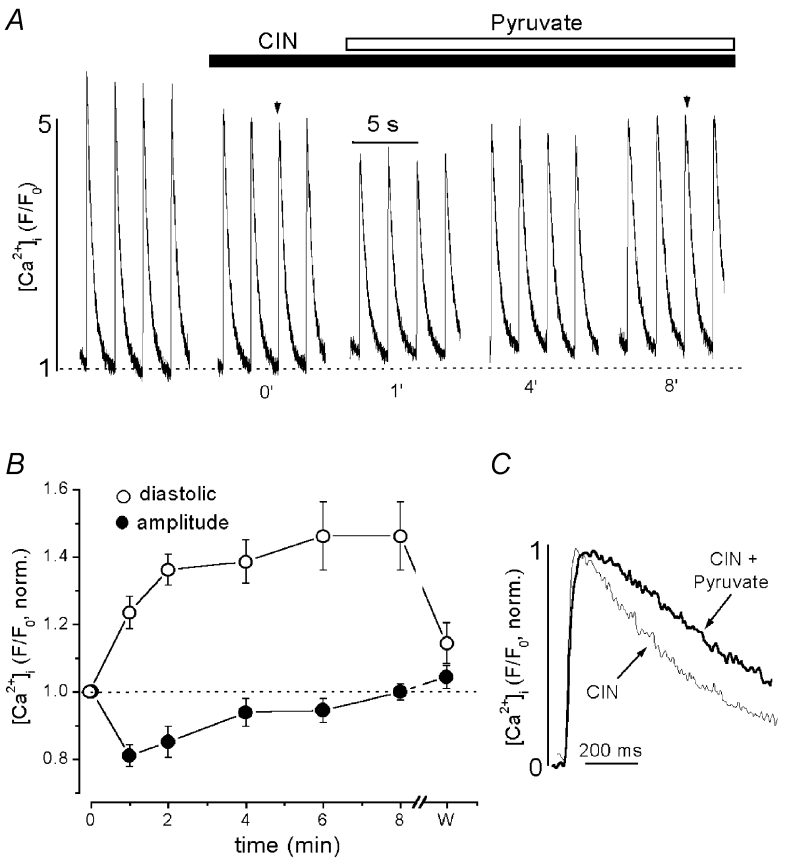

Figure 6. The effect of pyruvate on $[Ca^{2+}]_i$ transients in the presence of the inhibitor of mitochondrial monocarboxylate transport CIN

A, changes of $[Ca^{2+}]_i$ transients after application of 10 mM pyruvate in an intact cell pretreated with 0.5 mM CIN (time in min). *B*, average normalized data of pyruvate-mediated changes of diastolic $[Ca^{2+}]_i$ (○) and $[Ca^{2+}]_i$ transient amplitudes (●) in the presence of CIN. Time as in *A* (w; washout recorded 4 min after removal of pyruvate). *C*, examples of $[Ca^{2+}]_i$ transients recorded at the times indicated by arrows in *A* on an expanded time scale. $[Ca^{2+}]_i$ transients in the presence of CIN (thin line) and CIN + pyruvate (thick line) were normalized and superimposed.

of inhibition of nucleotide translocation by atractyloside (ATR; Klingenberg, 1989) was explored (Fig. 7). Again, original $[Ca^{2+}]_i$ traces (Fig. 7*A*) and averaged data (Fig. 7*B*) normalized to the control in the presence of ATR are presented. Pretreatment of cells with ATR (0.3 mM) for 5 min induced a modest, but statistically significant reduction of the $[Ca^{2+}]_i$ transient amplitude by 13 ± 2 % from 4.6 ± 0.4 to 4.0 ± 0.4 ($n = 6$; $P < 0.005$), without affecting diastolic $[Ca^{2+}]_i$ (Fig. 7*A*). The subsequent application of pyruvate produced a further decrease of the $[Ca^{2+}]_i$ transient amplitude by 21 ± 4 % from 4.0 ± 0.4 to 3.2 ± 0.4 (after 1 min of pyruvate exposure, $n = 6$; $P < 0.001$). This inhibitory effect of pyruvate reached a maximum within the first few minutes followed by a partial and incomplete recovery (Fig. 7*B*). Similar to CIN, ATR did not change the pyruvate-mediated elevation of diastolic $[Ca^{2+}]_i$ and prolongation of the rising phase of the $[Ca^{2+}]_i$ transient. Pyruvate increased diastolic $[Ca^{2+}]_i$ by 47 ± 12 % ($n = 6$) in the presence of ATR, which was not statistically different from control (57 ± 5 %, Fig. 1*B*). In the presence of ATR, pyruvate also increased the time-to-peak of the $[Ca^{2+}]_i$ transient by 135 % from 80 ± 12 ms to 190 ± 21 ms ($n = 6$; $P < 0.002$; Fig. 7*C*).

Inhibition of mitochondrial oxidative phosphorylation. Finally, we examined the effects of pyruvate on electrically evoked $[Ca^{2+}]_i$ transients in the presence of 4 mM cyanide (CN^-), which blocks mitochondrial ATP production by inhibition of the electron transport chain at the level of the cytochrome oxidase complex. Similar to CIN and ATR, CN^- inhibited the pyruvate-mediated augmentation of the $[Ca^{2+}]_i$ transient amplitude. In the presence of CN^-, pyruvate increased diastolic $[Ca^{2+}]_i$ and the time-to-peak of the $[Ca^{2+}]_i$ transient (data not shown).

Taken together, these results indicate that pyruvate increased the $[Ca^{2+}]_i$ transient amplitude, most probably through augmentation of the cytosolic phosphorylation potential due to mitochondrial pyruvate oxidation and an increase in the rate of ATP production.

Dependence of SR Ca^{2+} load on the [ATP]/[ADP] ratio in permeabilized myocytes

To examine the possibility that the cytosolic phosphorylation potential affects SR Ca^{2+} load, we studied the effects of varying the cytoplasmic [ATP]/[ADP] ratio (while $[P_i]$ was kept constant) on caffeine-induced Ca^{2+} release in saponin-permeabilized ventricular myocytes. Membrane permeabilization permits the study of SR function in its near-physiological membranous environment, while simultaneously allowing control of the cytoplasmic milieu with regard to ionic composition, pH and metabolic substrates. After permeabilization, the cells were placed in an internal solution containing 5 mM ATP and 0.01 mM ADP (free $[Ca^{2+}]$ and $[Mg^{2+}]$ were 100 nM and 1 mM, respectively) and stimulated by repeated (every 2 min) application of 20 mM caffeine (Fig. 8). The

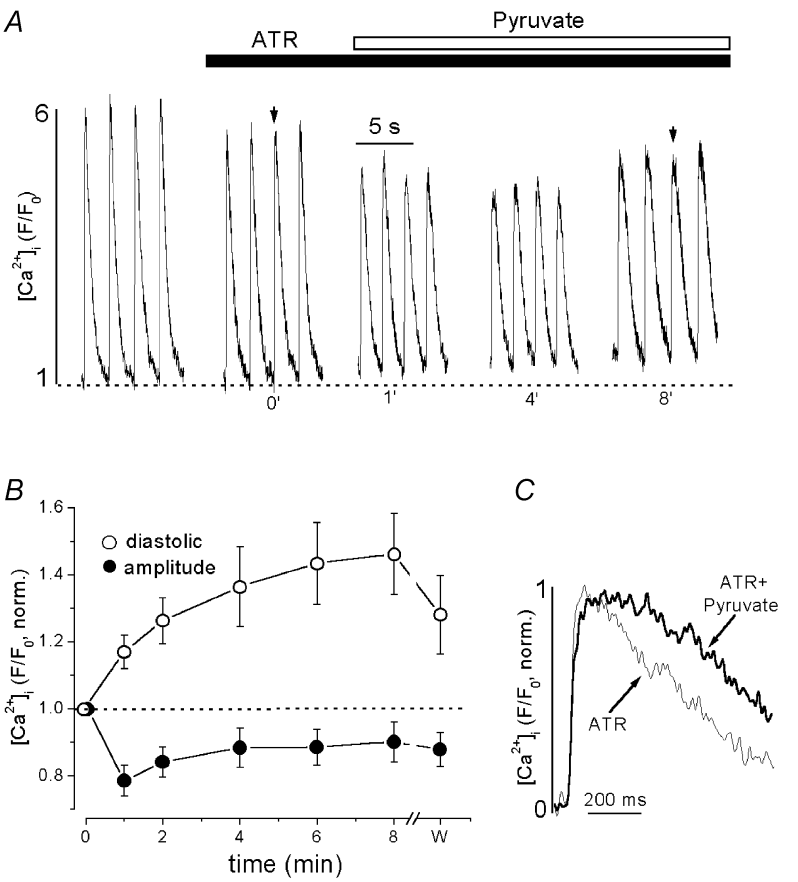

Figure 7. The effect of pyruvate on $[Ca^{2+}]_i$ transients in the presence of the inhibitor of mitochondrial nucleotide translocation ATR

A, changes of $[Ca^{2+}]_i$ transients after application of 10 mM pyruvate in an intact cell pretreated with 0.3 mM ATR (time in min). *B*, average normalized data of pyruvate-mediated changes of diastolic $[Ca^{2+}]_i$ (○) and $[Ca^{2+}]_i$ transient amplitudes (●) in the presence of ATR. Time as in *A* (w; washout recorded at 4 min after removal of pyruvate). *C*, examples of $[Ca^{2+}]_i$ transients recorded at the times indicated by arrows in *A* on an expanded time scale. The transients in the presence of ATR (thin line) and ATR + pyruvate (thick line) were normalized and superimposed.

amplitude of the caffeine-induced $[Ca^{2+}]_i$ transient was used as an index of SR Ca^{2+} load. Figure 8*A* shows representative linescan images and F/F_0 plots of Ca^{2+} release induced by application of 20 mM caffeine at different [ATP]/[ADP] ratios, while Fig. 8*B* shows the corresponding average data. Doubling of the [ATP]/[ADP] ratio by increasing [ATP] from 5 mM to 10 mM increased the amplitude of the caffeine-induced Ca^{2+} release from 2.6 ± 0.1 ($n = 10$) to 3.2 ± 0.1 ($n = 8$; $P < 0.05$) or by 24 %. This effect occurred rapidly (< 1 min) and was readily reversible. In contrast, reduction of the [ATP]/[ADP] ratio by increasing [ADP] from 0.01 mM to 0.2 mM significantly decreased the amplitude of Ca^{2+} release from 2.6 ± 0.1 ($n = 10$) to 0.9 ± 0.3 ($n = 6$; $P < 0.002$) or by 65 %. These results indicate that in our experimental conditions Ca^{2+} accumulation by the SR directly correlated with the cytosolic [ATP]/[ADP] ratio.

Pyruvate reduces the frequency of spontaneous Ca^{2+} sparks

The observation that, in the presence of the inhibitors of mitochondrial function (Figs 6 and 7), pyruvate caused a reduction of the amplitude together with an increase of the time-to-peak of the $[Ca^{2+}]_i$ transient suggested that pyruvate had additional, mitochondria-independent effects on SR Ca^{2+} release. To test this possibility we investigated the effects of pyruvate on spontaneous SR Ca^{2+} release (Ca^{2+} sparks) in permeabilized myocytes. To inhibit mitochondrial pyruvate uptake and ATP synthesis, CIN and oligomycin were added to the solution. Figure 9*A* shows representative linescan images from a permeabilized ventricular myocyte (upper panel) and the time course of changes in frequency and amplitude of spontaneous Ca^{2+} sparks (lower panel) under control conditions, after addition of 0.5 mM CIN and 1 μM oligomycin, after the subsequent application of 4 mM pyruvate and following washout of pyruvate. CIN and oligomycin had no significant effect on the frequency of Ca^{2+} sparks (9.2 ± 1.1 in control *vs.* 9.1 ± 0.6 sparks s^{-1} (100 μm)$^{-1}$ after adding CIN and oligomycin; $n = 8$) and Ca^{2+} spark amplitude ($\Delta F/F_0 = 1.15 \pm 0.05$ in control *vs* 1.00 ± 0.04 after adding CIN and oligomycin; $n = 8$; not statistically different). Subsequent addition of 4 mM pyruvate resulted in a 43 % inhibition of Ca^{2+} spark frequency (5.1 ± 0.7 sparks s^{-1} (100 μm)$^{-1}$; $n = 8$; $P < 0.002$). This effect was partially reversible upon washout of pyruvate. Furthermore,

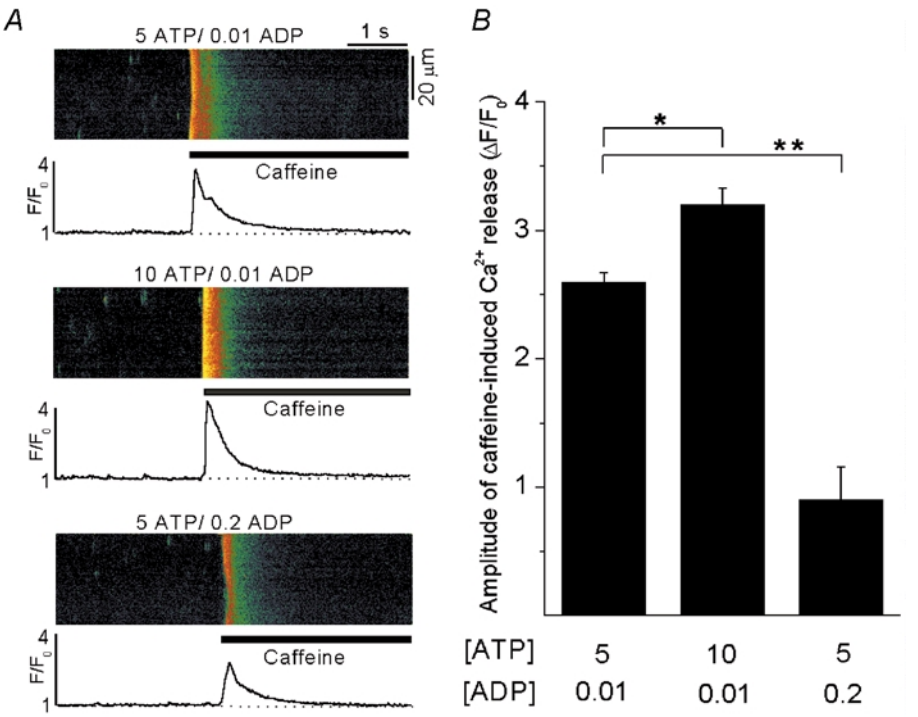

Figure 8. Effect of the [ATP]/[ADP] ratio on caffeine-induced Ca^{2+} release in saponin-permeabilized myocytes

A, confocal linescan images and corresponding F/F_0 plots of Ca^{2+} release induced by application of 20 mM caffeine under different [ATP]/[ADP] ratios of 500:1, 1000:1 and 25:1. F/F_0 plots were obtained by averaging the entire cellular fluorescence signal from the linescan images. The measurements of $[Ca^{2+}]_i$ were made from the same myocyte. In all experimental solutions free $[Ca^{2+}]$ and $[Mg^{2+}]$ were adjusted to 100 nM and 1 mM, respectively. In this set of experiments phosphocreatine and creatine phosphokinase were omitted from the internal solution. *B*, average amplitudes of caffeine-induced Ca^{2+} release under different [ATP]/[ADP] ratios. * Statistically different at $P < 0.05$; ** statistically different at $P < 0.002$.

pyruvate decreased the Ca^{2+} spark amplitude by 23 % from 1.00 ± 0.04 to 0.77 ± 0.03 ($n = 8$; $P < 0.05$). Figure 9*B* summarizes the effects of 0.5 mM CIN and 1 μM oligomycin as well as 4 mM pyruvate on the average frequency and peak amplitude of Ca^{2+} sparks. The same tendency of pyruvate to decrease Ca^{2+} spark frequency was also observed in the absence of CIN and oligomycin (data not shown).

In another set of experiments, putative changes of SR Ca^{2+} load in the presence of pyruvate were verified by application of caffeine (20 mM). Pyruvate (4 mM) increased the amplitude of the caffeine-induced Ca^{2+} release from 2.5 ± 0.1 to 2.8 ± 0.1 ($n = 5$; $P < 0.05$) or by 12 % (Fig. 9*C*). Thus, at constant $[Ca^{2+}]$, [ATP] and pH, pyruvate appeared to decrease spontaneous SR Ca^{2+} release through the RyR and, simultaneously, to increase SR Ca^{2+} load.

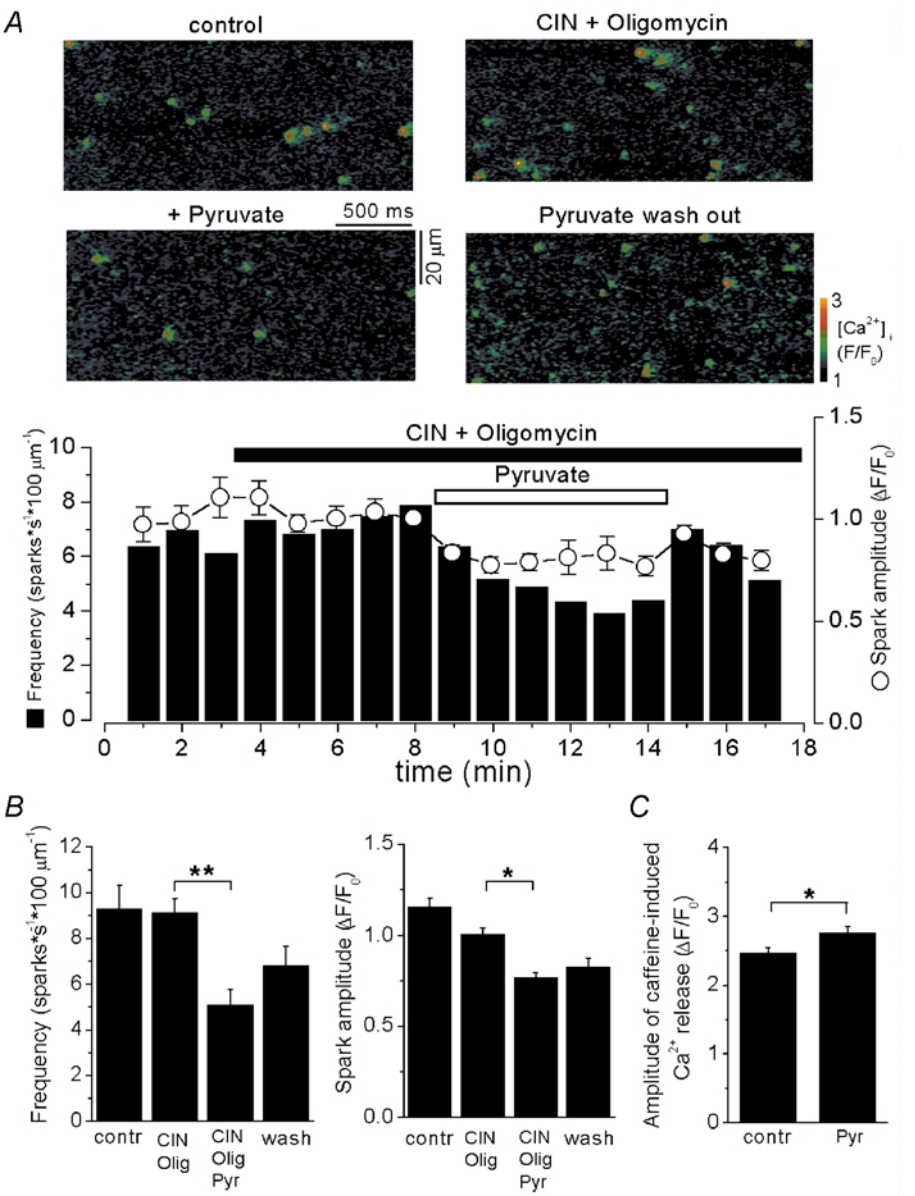

Figure 9. The effect of pyruvate on Ca^{2+} sparks in permeabilized myocytes

A, top: confocal linescan images showing Ca^{2+} sparks in control conditions, after addition of 0.5 mM CIN and 1 μM oligomycin, subsequent addition of 4 mM pyruvate and washout of pyruvate. Bottom: time course of changes in frequency and Ca^{2+} spark amplitude after addition of pyruvate in the presence CIN and oligomycin. Ca^{2+} spark frequency is expressed as the number of events per second measured along a scanned distance of 100 μm. *B*, average spark frequencies and amplitudes under control conditions, in the presence of CIN and oligomycin, and after addition and washout of pyruvate. *C*, average amplitudes of caffeine-induced (20 mM) $[Ca^{2+}]_i$ transients under control conditions and in the presence of pyruvate (4 mM). * Statistically different at $P < 0.05$ and ** statistically different at $P < 0.002$.

Pyruvate depresses RyR function

To test the possibility that the observed inhibitory effects of pyruvate on Ca^{2+} spark amplitude and frequency were associated with a direct inhibition of the RyR, we studied the effect of pyruvate on the activity of single RyR channels incorporated into planar lipid bilayers. After fusion of SR microsomes with the lipid membrane bilayer, single-channel currents were recorded using Cs^+ as the charge carrier. First, we characterized the biophysical and pharmacological properties of our RyR preparation. The conductance of the RyR channel, measured with a ramp depolarization protocol from −60 to +60 mV (24 mV s^{-1}) in symmetric ionic conditions (400 mM Cs^+ on both sides), was 606 ± 37 pS ($n = 12$, data not shown). Figure 10*A* illustrates the effect of increasing cytosolic (*cis*) [Ca^{2+}] on channel activity. Elevating *cis*[Ca^{2+}] resulted in an increase of the open probability (P_o) and mean open time of the channel. Half-maximal activation occurred at *cis*[Ca^{2+}] of 9.7 μM. At 100 μM *cis*[Ca^{2+}] RyR channels were fully activated with a P_o of 0.55 ± 0.06 ($n = 25$). The effect of ryanodine (5 μM) on RyR channel activity is illustrated in Fig. 10*B*. Ryanodine altered the gating properties of the channel by locking it in a sub-conductance state comprising 53 ± 5 % ($n = 3$) of the fully open state. Furthermore, caffeine (2 mM, Fig. 10*C*) and ATP (5 mM, see Fig. 11*E*) increased, whereas Mg^{2+} (2 mM, Fig. 10*C*) decreased RyR activity. Based on these properties the channels were identified as typical cardiac RyRs (Meissner, 1994).

Figure 11*A* shows the effect of pyruvate on RyR channel activity recorded in the presence of 3 μM *cis*[Ca^{2+}]. On average the addition of 1 mM pyruvate to the cytosolic side of the channel resulted in a reduction of P_o by 59 ± 10 %. P_o was reduced from 0.133 ± 0.019 under control conditions to 0.054 ± 0.013 in the presence of 1 mM pyruvate (Fig. 11*D*, $n = 6$; $P < 0.002$). This effect reached a maximum after 2–3 min following addition of pyruvate and was completely reversible (Fig. 11*A*). Pyruvate added to the lumenal side had no effect on RyR channel activity. Pyruvate did not change the amplitude of the single channel current, but slightly (~14 %) decreased the mean open time of RyR channels from 2.7 ± 0.3 ms under control conditions (*cis*[Ca^{2+}] = 3 μM) to 2.3 ± 0.2 ms in the presence of 1 mM pyruvate ($n = 6$; $P < 0.05$). The open time distributions from a representative channel are illustrated in Fig. 11*B*. Because pyruvate had no profound

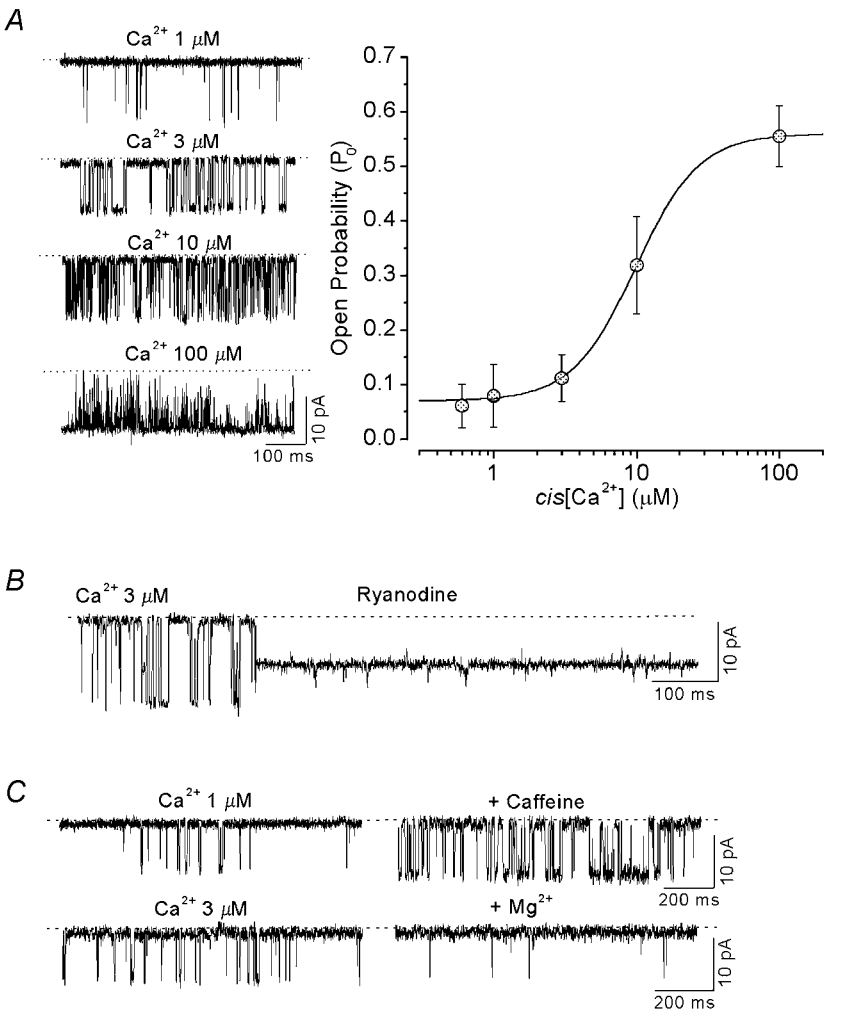

Figure 10. Properties of single RyR channels incorporated into planar lipid bilayer

A, recordings of RyR channel currents activated by different *cis*[Ca^{2+}] (left panel). The dotted line indicates the closed state of the channel. Dependence of RyR open probability (P_o) on *cis*[Ca^{2+}] (right panel). Average data were fitted by a Hill equation with $K_a = 9.7$ μM and $n = 1.8$. *B*, effect of 5 μM ryanodine on RyR channel activity. *C*, top: effect of 2 mM caffeine (*cis*[Ca^{2+}] = 1 μM) on RyR channel activity. Bottom: effect of 2 mM Mg^{2+} (*cis*[Ca^{2+}] = 3 μM).

effect on the mean open time of the channels, it seemed to reduce P_o predominantly by decreasing the frequency of channel openings. Taken together, these results indicate that pyruvate inhibited channel activity by interactions with the RyR or a closely associated regulatory protein from the cytosolic side.

Because in intact cells pyruvate increased both diastolic $[Ca^{2+}]_i$ and mitochondrial ATP production, we investigated whether changes in *cis*$[Ca^{2+}]$ or *cis*[ATP] could alter the inhibitory effect of pyruvate on RyR channel activity. Figure 11*C* shows the effect of pyruvate on RyR channels activated by two different concentrations of cytosolic Ca^{2+} (threshold (0.6 μM) and half-maximum (10 μM) concentration, see Fig. 10*A*). In the two cases, pyruvate caused a quantitatively similar inhibition of channel activity (Fig. 11*D*). Pyruvate (1 mM) decreased the P_o by 57 ± 8 % (n = 5) at 0.6 μM Ca^{2+} and by 66 ± 6 % (n = 5) at 10 μM Ca^{2+}. Figure 11*D* summarizes the effect of pyruvate on the P_o of RyR channels at various *cis*$[Ca^{2+}]$. For the range between 0.6 and 10 μM *cis*$[Ca^{2+}]$, pyruvate reduced P_o by about the same degree (60–70 %).

Figure 11*E* shows an experiment in which the effect of pyruvate (1 mM) on RyR channel activity was studied under control conditions (1 μM *cis*$[Ca^{2+}]$) and following addition of ATP (5 mM) to the cytosolic side of the channel. In this experiment two channels were present in the lipid bilayer. Under control conditions, pyruvate reversibly reduced P_o on average by 59 ± 10 % (n = 6). Addition of ATP dramatically increased channel activity by a factor of 9. In the presence of ATP, pyruvate again inhibited channel activity by 51 ± 11 % (n = 4; statistically not different from control).

In summary, these results suggest that pyruvate has a direct inhibitory effect on the RyR SR Ca^{2+} release channel which is largely independent of $[Ca^{2+}]$ and [ATP]. This observation is consistent with the finding that pyruvate

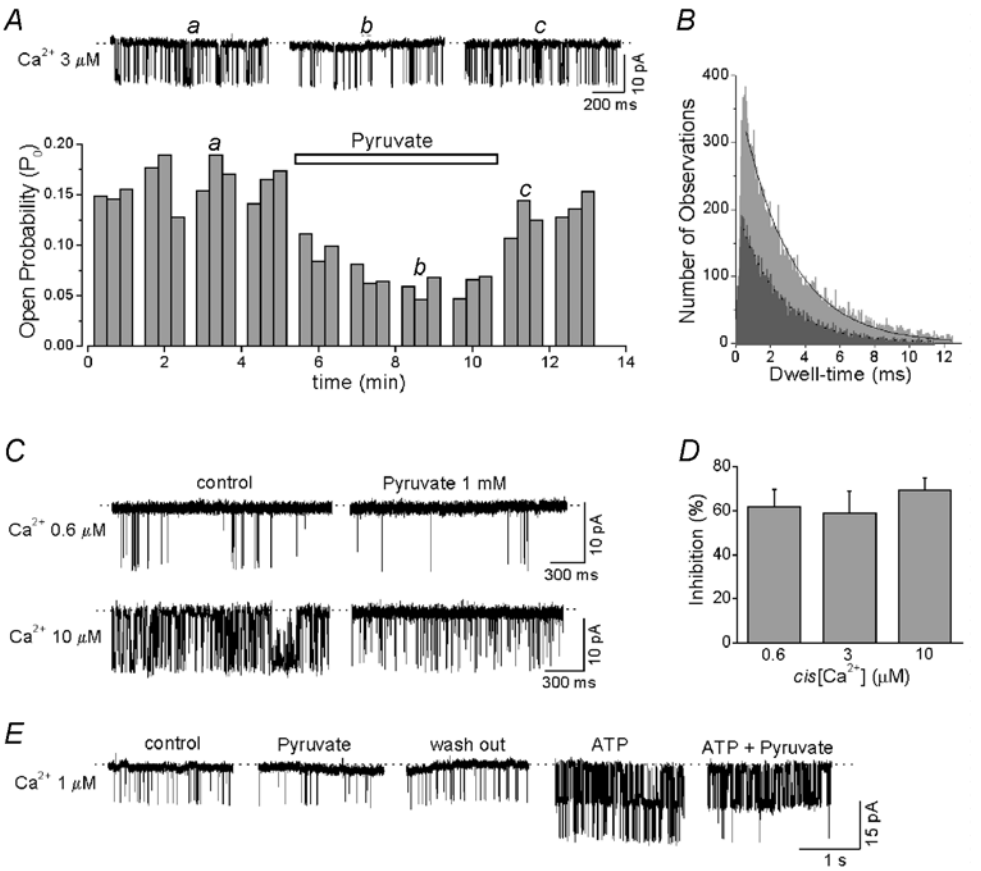

Figure 11. Effect of pyruvate on RyR channel activity

A, RyR channel currents and P_o under control condition (*a*), after adding 1 mM pyruvate (*b*), and after washout of pyruvate (*c*). *B*, open time distributions for a representative RyR channel in control conditions (light grey) and in the presence of pyruvate (dark grey). Experimental data were fitted by a single exponential function from which mean open time was derived. *C*, effect of 1 mM pyruvate on RyR channels activated by different *cis*$[Ca^{2+}]$. *D*, relationship between *cis*$[Ca^{2+}]$ and degree of reduction of P_o by pyruvate. *E*, RyR channel current recordings under control conditions, after adding 1 mM pyruvate, after washout of pyruvate, after adding 5 mM ATP and after subsequent re-addition of 1 mM pyruvate.

also reduced the frequency and amplitude of spontaneous Ca^{2+} sparks.

DISCUSSION

The purpose of the present study was to elucidate the mechanisms underlying the inotropism of the glycolytic product and Krebs cycle substrate pyruvate in rat ventricular myocytes. The main findings are: (1) pyruvate increased the action potential-induced $[Ca^{2+}]_i$ transient as a result of enhanced SR Ca^{2+} load; (2) pyruvate increased diastolic $[Ca^{2+}]_i$ due to intracellular acidification; and (3) pyruvate decreased spontaneous Ca^{2+} release from the SR (Ca^{2+} sparks) by direct inhibition of the activity of SR Ca^{2+} release channels (RyRs). The pyruvate-mediated slowing of the upstroke of the $[Ca^{2+}]_i$ transient was most probably due to depression of RyRs caused by a direct inhibitory effect of pyruvate. Elevation of SR Ca^{2+} content was probably mediated by increased SR Ca^{2+} pumping due to augmentation of the cytosolic [ATP]/[ADP] ratio as a result of mitochondrial ATP synthesis, while a reduction of the SR Ca^{2+} leak due to a direct inhibition of RyRs by pyruvate might have contributed to this effect.

Pyruvate decreases pH_i and increases resting $[Ca^{2+}]_i$

Pyruvate is imported into cardiac myocytes together with a proton by means of a sarcolemmal H^+-monocarboxylate symporter (Poole & Halestrap, 1993). The uptake of pyruvate, therefore, is likely to lead to acidification of the cytoplasm. Consistent with this notion, we found that extracellular pyruvate caused sustained intracellular acidification. In parallel with the pyruvate-induced acidification we observed an increase in diastolic $[Ca^{2+}]_i$. It is likely that this increase of $[Ca^{2+}]_i$ was a direct consequence of cytoplasmic acidification and not a pyruvate-specific effect on resting $[Ca^{2+}]_i$. This conclusion is drawn from the observation that changes of pH_i and diastolic $[Ca^{2+}]_i$ exhibited similar time courses. Moreover, similar increases of diastolic $[Ca^{2+}]_i$ occurred regardless whether pH_i was lowered by application of pyruvate or D-lactate.

Several hypotheses have been put forward over the years to explain the parallel changes in $[Ca^{2+}]_i$ and pH_i (for reference see Bers, 2001). The most common explanation refers to the competition between Ca^{2+} and H^+ for shared cytoplasmic binding sites. According to this explanation, acidification results in an increase of diastolic $[Ca^{2+}]_i$ because of a decrease of the cytoplasmic Ca^{2+} buffering capacity. Another possibility is that pyruvate alters Ca^{2+} extrusion through changes in pH_i. Acidification of the cytosol increases $[Na^+]_i$ by proton extrusion via Na^+–H^+ exchange. Increased levels of $[Na^+]_i$, in turn, can alter the activity of Na^+–Ca^{2+} exchange (Bountra & Vaughan-Jones, 1989; Harrison *et al.* 1992) and, together with a direct inhibition of Na^+–Ca^{2+} exchange by low pH (Philipson *et al.* 1982), cause an increase of SR Ca^{2+} load and $[Ca^{2+}]_i$ transient amplitude. Thus, the question arose whether the pyruvate effects on the $[Ca^{2+}]_i$ transient amplitude could also be the direct consequence of cytoplasmic acidification. It has been reported that acidosis indeed increased the $[Ca^{2+}]_i$ transient amplitude (Hulme & Orchard, 1998; Balnave & Vaughan-Jones, 2000) despite a reduced activity of the SR Ca^{2+}-ATPase at lower pH (Fabiato & Fabiato, 1978; Mandel *et al.* 1982). There are, however, several lines of evidence that the pyruvate effect on the $[Ca^{2+}]_i$ transient amplitude was not caused by intracellular acidification in our study. First, unlike pyruvate, D-lactate did not increase the amplitude of the electrically evoked $[Ca^{2+}]_i$ transient although the two compounds induced the same degree of acidification. Second, the time course of the pyruvate-mediated acidification (which followed closely the development of the increase of diastolic $[Ca^{2+}]_i$) differed clearly from the time course of the changes of $[Ca^{2+}]_i$ transient amplitude, suggesting that two different mechanisms were involved. Third, in experiments with inhibitors of mitochondrial function, pyruvate produced a transient decrease instead of an increase of $[Ca^{2+}]_i$ transient amplitude. Fourth, application of pyruvate during inhibition of Na^+–H^+ exchange with cariporide increased the $[Ca^{2+}]_i$ transient amplitude by the same amount as under control conditions. This finding suggests that the positive inotropic effect of pyruvate could not be explained by elevated $[Na^+]_i$ due to increased Na^+–H^+ exchange activity. Thus, neither acidosis *per se* nor putative acidosis-induced elevations of $[Na^+]_i$ were sufficient to account for the pyruvate-mediated increases in $[Ca^{2+}]_i$ transient amplitude.

Pyruvate augments the amplitude of the $[Ca^{2+}]_i$ transient by increasing SR Ca^{2+} load

Pyruvate (10 mM) increased the amplitude of action potential-induced $[Ca^{2+}]_i$ transients by about 50 %, very similar to the maximum increases reported in earlier studies in rat ventricular myocytes (Martin *et al.* 1998; Mellors *et al.* 1999). In the light of the sequence of events during cardiac excitation–contraction coupling, pyruvate may have various targets ultimately leading to an enhanced $[Ca^{2+}]_i$ transient: (1) pyruvate could increase Ca^{2+} entry through sarcolemmal L-type Ca^{2+} channels thus enhancing the trigger for Ca^{2+} release from the SR; (2) pyruvate could increase the Ca^{2+} uptake and/or load of the SR; and (3) pyruvate could have a direct stimulatory effect on SR Ca^{2+} release channels.

With regard to the first possibility, we have shown previously that pyruvate does not affect the amplitude of the L-type Ca^{2+} current in cat cardiac myocytes (Hüser *et al.* 2000). Furthermore, pyruvate inhibited, rather than stimulated, the activity of cardiac RyRs (see below) leaving increased SR Ca^{2+} content as the most likely explanation for the augmented $[Ca^{2+}]_i$ transient. Indeed, as directly shown by caffeine applications, pyruvate exposure resulted in an increase of SR Ca^{2+} load by ~30 %. Elevated SR Ca^{2+}

load could result from increased SR Ca^{2+} pumping, from a reduced SR Ca^{2+} leak or from a combination of both. According to our experimental data, the latter possibility appears to be the most likely since we obtained evidence for both increased SR Ca^{2+} uptake (due to an increased [ATP]/[ADP] ratio) and decreased SR Ca^{2+} leak (due to a reduced P_o of RyRs), as discussed below.

The pyruvate-induced elevation of SR Ca^{2+} load is mediated by the mitochondria

To assess the role of the mitochondria in the effects of pyruvate on $[Ca^{2+}]_i$, we used 0.5 mM CIN to selectively inhibit mitochondrial pyruvate uptake. It has been shown that at a submillimolar (0.6 mM) concentration CIN does not affect the sarcolemmal H^+-monocarboxylate symporter (Bünger & Mallet, 1993) and can therefore be considered mitochondria specific. This allowed us to experimentally separate mitochondrial from cytosolic pyruvate effects. CIN completely abolished the stimulatory effect of pyruvate on the $[Ca^{2+}]_i$ transient amplitude. By contrast, CIN did not prevent the pyruvate-mediated elevation of diastolic $[Ca^{2+}]_i$ and the slowing of the upstroke of the $[Ca^{2+}]_i$ transient, suggesting that CIN indeed selectively blocked the mitochondrial monocarboxylate transporter and further emphasizing that the latter effects entailed different, mitochondria-independent mechanisms. The results are consistent with previous findings from whole hearts and single cardiac myocytes showing that the positive inotropic effect of pyruvate was strongly inhibited by submillimolar concentrations of CIN (Martin *et al.* 1998; Mallet & Sun 1999).

To substantiate the role of the mitochondria in the pyruvate-mediated inotropism, we used pharmacological inhibitors of the adenine nucleotide (ATP–ADP) exchanger of the inner mitochondrial membrane, ATR, and the electron transport chain, CN^-. Inhibition of mitochondrial ATP transport to the cytosol by ATR completely abolished the stimulatory effect of pyruvate on the $[Ca^{2+}]_i$ transient. Moreover, CN^- also inhibited the positive inotropic effect of pyruvate. Thus, uptake into the mitochondria via the mitochondrial monocarboxylate transporter, oxidative phosphorylation, and ATP exchange between the mitochondria and the cytosol are absolutely required for the positive inotropic effect of pyruvate. In addition, pyruvate increased mitochondrial redox potential as evidenced by the decrease of FAD-linked autofluorescence, suggesting the following sequence of events for mitochondrial pyruvate actions. First, pyruvate enters the mitochondria through the mitochondrial monocarboxylate transporter where it is oxidatively decarboxylated to acetyl coenzyme A and fed into the Krebs cycle. This will ultimately result in an elevation of the mitochondrial reducing equivalent ($FADH_2$/FAD and NADH/NAD^+ ratios) and therefore in an increase of the driving force for ATP production. Finally, ATP synthesized in the mitochondrial matrix, is transferred to the cytosol via the adenine nucleotide exchanger, which results in an increase of the [ATP]/[ADP] ratio.

It is generally accepted, that the SR Ca^{2+}-ATPase is regulated thermodynamically (i.e. by ΔG_{ATP}) as well as kinetically (i.e. via changes of ATP hydrolysis products; for review see Kodama, 1985). The dependence of cardiac SR Ca^{2+} uptake on energy supply has also been demonstrated in experiments with skinned myocytes (Wimsatt *et al.* 1990), skinned multicellular preparations (Xiang & Kentish, 1995) and SR vesicles (Shannon & Bers, 1997). Moreover, the activity of the SR Ca^{2+} pump also depends on the removal of ATP hydrolysis products, especially ADP. It has been shown that accumulation of ADP in the proximity of the SR Ca^{2+}-ATPase slows down its activity and impairs Ca^{2+} uptake (Inesi & de Meis, 1989; Macdonald & Stephenson, 2001). Therefore, any change of the cytosolic [ATP]/[ADP] ratio is expected to affect the efficiency of the SR Ca^{2+} pump and thus SR Ca^{2+} load (provided that the SR Ca^{2+} leak remains unchanged). In line with this notion we found that changes of the [ATP]/[ADP] ratio significantly affected SR Ca^{2+} content in permeabilized myocytes. Elevation of [ATP] at constant [ADP] increased, whereas elevation of [ADP] at constant [ATP] decreased SR Ca^{2+} load. This result is in agreement with recent reports indicating that pyruvate increased the Ca^{2+} gradient between the SR and the cytosol (Chen *et al.* 1998) or SR Ca^{2+} turnover (Mallet & Bünger, 1994; Mallet & Sun, 1999) secondary to an increase of the cytosolic [ATP]/[ADP] ratio.

Our finding that, in permeabilized myocytes, SR Ca^{2+} content is directly affected by the cytosolic [ATP]/[ADP] ratio (at millimolar ATP concentrations) appears to be at variance with recent work from Yang & Steele (2001). These authors have shown that a reduction of [ATP] from 5 mM to 1 mM increased rather than decreased SR Ca^{2+} content. It was suggested that this was caused by a decreased SR Ca^{2+} leak at constant Ca^{2+} uptake since the activity of the RyR is thought to be much more sensitive to a reduction of [ATP] than the activity of the SR Ca^{2+} pump. The apparent discrepancy between the findings of Yang & Steele (2001) and ours, however, may be explained by the different experimental conditions. Yang & Steele (2001) studied the effects of [ATP] on SR Ca^{2+} release in the presence of phosphocreatine (10 mM) whereas our experiments were conducted in the absence of phosphocreatine. [Phosphocreatine] and [ATP] are kept at equilibrium through the creatine kinase reaction (Wallimann *et al.* 1992). Therefore, it is likely that in the presence of phosphocreatine a relatively high [ATP]/[ADP] ratio could be maintained close to the SR Ca^{2+} uptake and/or release sites making firm conclusions on the dependence of SR Ca^{2+} regulation on cytoplasmic [ATP] and [ADP] difficult. Furthermore, recent work indicates

that in the presence of physiological concentrations of Mg^{2+}, the RyR becomes relatively insensitive to changes of [ATP] in the range 1–5 mM. A slight inhibition of channel activity is observed only after complete removal of ATP (Xu *et al.* 1996; Copello *et al.* 2002). Thus, it is conceivable that in our experiments changing [ATP] failed to exert any direct effects on RyRs and Ca^{2+} leak from the SR.

A different situation might arise when cytoplasmic [ATP] is reduced to the submillimolar range, as may occur during ischaemia/anoxia. The activities of both the RyR and the SR Ca^{2+} pump may be substantially compromised under these conditions. Strong inhibition of the RyR would outweigh the rather weak inhibition of the SR Ca^{2+} pump, resulting in net accumulation of Ca^{2+} in the SR (Yang & Steele, 2000, 2001; Smith & O'Neill, 2001).

Direct inhibitory effect of pyruvate on SR Ca^{2+} release channels

Under control conditions some cells responded to pyruvate exposure with a transient reduction in $[Ca^{2+}]_i$ transient amplitude (e.g. Figs 1*A* and 2). This inhibitory effect became more profound when the positive inotropic effect of pyruvate was abolished by inhibitors of mitochondrial function (CIN and ATR). A possible explanation for such a reduction of the $[Ca^{2+}]_i$ transient amplitude is that pyruvate might have additional, mitochondria-independent inhibitory effects on SR Ca^{2+} release. Similar changes of SR Ca^{2+} release have been previously described for tetracaine, an inhibitor of the RyR channel (Györke *et al.* 1997; Overend *et al.* 1997). The inhibition of RyR channels causes only transient suppression of Ca^{2+} release from the SR, since increased SR Ca^{2+} content (due to decreased SR Ca^{2+} leak) will lead to gradual recovery of the $[Ca^{2+}]_i$ transient amplitude (due to activation of release channels by Ca^{2+} on the luminal side of the channel).

Three lines of evidence support the notion of a direct inhibitory effect of pyruvate on SR Ca^{2+} release. First, pyruvate slowed the rising phase of the $[Ca^{2+}]_i$ transient. This effect was the same whether mitochondrial pyruvate metabolism was inhibited or not. Furthermore, this change in the kinetics of the $[Ca^{2+}]_i$ transient did not seem to be related to pH_i *per se* since it was not observed during acidification caused by D-lactate. Second, pyruvate reduced the amplitude and the frequency of spontaneous Ca^{2+} sparks in permeabilized rat ventricular myocytes, i.e. under conditions where RyR-mediated SR Ca^{2+} release could be studied with bulk cytosolic $[H^+]$, $[Ca^{2+}]$, [ATP] and [pyruvate] maintained at known levels. Third, pyruvate reduced the P_o of isolated RyR release channels in planar lipid bilayers. The latter observation represents the most compelling evidence for a direct inhibitory effect of pyruvate on SR Ca^{2+} release. Analysis of the single channel data revealed that the unitary conductance of the RyR remained unaffected and that P_o was reduced primarily by a decrease of the frequency of single channel openings. Mean open time was only slightly affected. Furthermore, the inhibitory effect of pyruvate was independent of cytosolic $[Ca^{2+}]$ and [ATP]. Therefore, the interaction of pyruvate with the RyR (or an ancillary protein) is not related to the Ca^{2+} and adenine nucleotide binding sites of the RyR. These findings have important implications for the physiology of pyruvate actions. They suggest that neither the inotropic nor the metabolic state of the cell will affect the ability of pyruvate to inhibit SR Ca^{2+} release.

Direct modulation of RyR function by glycolytic intermediates is not unprecedented. Kermode *et al.* (1998) reported that fructose 1,6-bisphosphate and, to a lesser extent, fructose 6-phosphate, glucose 6-phosphate and glucose 1-phosphate activated cardiac RyRs in planar lipid bilayers and stimulated ryanodine binding to cardiac RyRs. Whether modulation of RyRs by either sugar phosphates or pyruvate involves direct binding to the RyR itself or to some tightly associated ancillary protein remains to be determined. Nonetheless, the results indicate that pyruvate affects SR Ca^{2+} turnover not only through mitochondria-dependent ATP production, but also through direct inhibition of SR Ca^{2+} release channels.

Possible physiological and clinical relevance

Plasma and bulk cytosolic concentrations of pyruvate have been reported to be in the submillimolar range (~0.1–0.3 mM; Mallet, 2000), clearly lower than the concentrations used in the present (1–10 mM) as well as in many previous studies (up to 20 mM). Pyruvate, however, does not appear to be distributed homogeneously throughout the cytosol nor is it freely diffusible. Metabolic studies in isolated hearts suggest the presence of at least two cytosolic pyruvate pools that do not exchange readily. The first pyruvate pool is generated by glycolysis, whereas the second pool is derived from exogenous pyruvate that is oxidized or transaminated (Damico *et al.* 1996). This subcellular compartmentalization of pyruvate may be due to the differential distribution of glycolytic enzymes as compared to glutamate–pyruvate transaminase or the mitochondria. Thus, it is possible that glycolytically derived pyruvate within these diffusion-limited microcompartments reaches much higher concentrations than in the bulk cytosol. Furthermore, even submillimolar concentrations of pyruvate (0.5 mM) exerted strong inhibitory effects on RyRs (reduction of P_o by ~25 %; A. K. Zima, J. Kockskämper, R. Mejia-Alvarez & L. A. Blatter, unpublished observations). Therefore, it is likely that under physiological conditions changes in glycolytic flux and thus local pyruvate concentration modulate RyR gating and SR Ca^{2+} release.

As to the positive inotropic effect of pyruvate, supraphysiological concentrations (~5–10 mM) seem to be required to elicit pronounced effects on cardiac function (Mallet, 2000). At a physiological concentration of 0.2 mM, pyruvate only slightly improved cardiac performance

(Bünger *et al.* 1989). Likewise, 2 mM pyruvate was unable to increase $[Ca^{2+}]_i$ transients and cell shortening in isolated ventricular myocytes (Martin *et al.* 1998). Thus, the beneficial effects of pyruvate may be restricted to the supraphysiological concentration range. Nevertheless, increased pyruvate metabolism brought about by administration of supraphysiological concentrations of pyruvate or stimulation of pyruvate oxidation by dichloroacetate has yielded encouraging results in heart failure patients (Bersin *et al.* 1994; Hermann *et al.* 1999) suggesting that it is worth pursuing the concept of pyruvate inotropism and of metabolic inotropism in general.

As outlined above, a growing body of evidence indicates that pyruvate (at least at supraphysiological concentrations) exerts beneficial effects on the heart. On the other hand, studies from our laboratory suggest that high concentrations of pyruvate (10 mM) can also be pro-arrhythmogenic by inducing Ca^{2+} alternans in atrial and ventricular myocytes from the cat heart (Hüser *et al.* 2000; Kockskämper & Blatter, 2002; Blatter *et al.* 2003). Indeed, a subset of cells in this study also exhibited transient Ca^{2+} alternans upon pyruvate application albeit to only a small degree (e.g. Fig. 2, 2 min mark). A recent report by Diaz and coworkers suggests that Ca^{2+} alternans may be elicited by simple depression of RyRs (Diaz *et al.* 2002). Thus, by direct inhibition of RyRs and, possibly, acidification and/or feedback inhibition of glycolysis, pyruvate may be able to generate Ca^{2+} alternans in cardiac myocytes. In ventricular myocytes pyruvate-induced alternans was less frequent and less severe than in atrial myocytes. Furthermore, during prolonged exposure of ventricular cells to pyruvate the positive inotropic effect prevailed, whereas in atrial myocytes prolonged pyruvate treatment did not result in any beneficial effects but rather worsened the Ca^{2+} alternans (A. K. Zima, J. Kockskämper, R. Mejia-Alvarez & L. A. Blatter, unpublished observations). Therefore, in ventricular myocytes pyruvate appears to exert predominantly beneficial effects (positive inotropy), whereas in atrial myocytes mainly adverse effects (Ca^{2+} alternans) are observed. The reason for this apparent cell type-specific difference in pyruvate action is unclear at present. It may possibly be related to the mitochondria, however. In atrial myocytes only ~20–25 % of cell volume is occupied by mitochondria as compared to ~30–37 % in ventricular myocytes (see Bers, 2001). Assuming that mitochondrial metabolism of pyruvate is important for its beneficial effects, this difference in mitochondrial abundance might explain why the adverse effects have the upper hand in atrial myocytes and why the beneficial effects prevail in ventricular cells. Although extrapolation to the clinical situation is notoriously difficult, some caution as to possible adverse side effects of supraphysiological pyruvate concentrations is at least warranted.

REFERENCES

Balnave CD & Vaughan-Jones RD (2000). Effect of intracellular pH on spontaneous Ca^{2+} sparks in rat ventricular myocytes. *J Physiol* **528**, 25–37.

Baudet S, Hove-Madsen L & Bers DM (1994). How to make and use calcium-specific mini- and microelectrodes. *Methods Cell Biol* **40**, 93–113.

Bers DM (2001). *Excitation–Contraction Coupling and Cardiac Contractile Force*, 2nd edn. Kluwer Academic Publishers, Dordrecht, The Netherlands.

Bers DM, Lederer WJ & Berlin JR (1990). Intracellular Ca transients in rat cardiac myocytes: role of Na–Ca exchange in excitation-contraction coupling. *Am J Physiol* **258**, C944–954.

Bersin RM, Wolfe C, Kwasman M, Lau D, Klinski C, Tanaka K, Khorrami P, Henderson GN, de Marco T & Chatterjee K (1994). Improved hemodynamic function and mechanical efficiency in congestive heart failure with sodium dichloroacetate. *J Am Coll Cardiol* **23**, 1617–1624.

Blatter LA, Kockskämper J, Sheehan KA, Zima AV, Hüser J & Lipsius SL (2003). Local calcium gradients during excitation–contraction coupling and alternans in atrial myocytes. *J Physiol* **546**, 19–31.

Blatter LA & McGuigan JA (1991). Intracellular pH regulation in ferret ventricular muscle. The role of Na–H exchange and the influence of metabolic substrates. *Circ Res* **68**, 150–161.

Bountra C & Vaughan-Jones RD (1989). Effect of intracellular and extracellular pH on contraction in isolated mammalian cardiac muscle. *J Physiol* **418**, 163–187.

Bünger R & Mallet RT (1993). Mitochondrial pyruvate transport in working guinea-pig heart. Work-related *vs.* carrier-mediated control of pyruvate oxidation. *Biochim Biophys Acta* **1151**, 223–236.

Bünger R, Mallet RT & Hartman DA (1989). Pyruvate-enhanced phosphorylation potential and inotropism in normoxic and postischemic isolated working heart. Near-complete prevention of reperfusion contractile failure. *Eur J Biochem* **180**, 221–233.

Chen W, London R, Murphy E & Steenbergen C (1998). Regulation of the Ca^{2+} gradient across the sarcoplasmic reticulum in perfused rabbit heart. A ^{19}F nuclear magnetic resonance study. *Circ Res* **83**, 898–907.

Cheng H, Song LS, Shirokova N, Gonzalez A, Lakatta EG, Rios E & Stern MD (1999). Amplitude distribution of calcium sparks in confocal images: theory and studies with an automatic detection method. *Biophys J* **76**, 606–617.

Choi HS, Trafford AW, Orchard CH & Eisner DA (2000). The effect of acidosis on systolic Ca^{2+} and sarcoplasmic reticulum calcium content in isolated rat ventricular myocytes. *J Physiol* **529**, 661–668.

Copello JA, Barg S, Sonnleitner A, Porta M, Diaz-Sylvester P, Fill M, Schindler H & Fleischer S (2002). Differential activation by Ca^{2+}, ATP and caffeine of cardiac and skeletal muscle ryanodine receptors after block by Mg^{2+}. *J Membr Biol* **187**, 51–64.

Damico LA, White LT, Yu X & Lewandowski ED (1996). Chemical *versus* isotopic equilibrium and the metabolic fate of glycolytic end products in the heart. *J Mol Cell Cardiol* **28**, 989–999.

de Hemptinne A, Marrannes R & Vanheel B (1983). Influence of organic acids on intracellular pH. *Am J Physiol* **245**, C178–183.

Diaz ME, Eisner DA & O'Neill SC (2002). Depressed ryanodine receptor activity increases variability and duration of the systolic Ca^{2+} transient in rat ventricular myocytes. *Circ Res* **91**, 553–555.

Endo M & Kitazawa T (1978). E–C coupling studies in skinned cardiac fibres. In *Biophysical Aspects of Cardiac Muscle*, ed. Morad M, pp. 307–327. Academic, New York.

Fabiato A & Fabiato F (1978). Effects of pH on the myofilaments and the sarcoplasmic reticulum of skinned cells from cardiac and skeletal muscles. *J Physiol* **276**, 233–255.

Györke S, Lukyanenko V & Györke I (1997). Dual effects of tetracaine on spontaneous calcium release in rat ventricularmyocytes. *J Physiol* **500**, 297–309.

Harrison SM, Frampton JE, McCall E, Boyett MR & Orchard CH (1992). Contraction and intracellular Ca^{2+}, Na^{+}, and H^{+} during acidosis in rat ventricular myocytes. *Am J Physiol* **262**, C348–357.

Hasenfuss G, Maier LS, Hermann HP, Lüers C, Hunlich M, Zeitz O, Janssen PM & Pieske B (2002). Influence of pyruvate on contractile performance and Ca^{2+} cycling in isolated failing human myocardium. *Circulation* **105**, 194–199.

Hassinen I & Chance B (1968). Oxidation–reduction properties of the mitochondrial flavoprotein chain. *Biochem Biophys Res Commun* **31**, 895–900.

Hermann HP, Pieske B, Schwarzmüller E, Keul J, Just H & Hasenfuss G (1999). Haemodynamic effects of intracoronary pyruvate in patients with congestive heart failure: an open study. *Lancet* **353**, 1321–1323.

Hermann HP, Zeitz O, Keweloh B, Hasenfuss G & Janssen PM (2000). Pyruvate potentiates inotropic effects of isoproterenol and Ca^{2+} in rabbit cardiac muscle preparations. *Am J Physiol Heart Circ Physiol* **279**, H702–708.

Hulme JT & Orchard CH (1998). Effect of acidosis on Ca^{2+} uptake and release by sarcoplasmic reticulum of intact rat ventricular myocytes. *Am J Physiol Heart Circ Physiol* **275**, H977–987.

Hüser J, Wang YG, Sheehan KA, Cifuentes F, Lipsius SL & Blatter LA (2000). Functional coupling between glycolysis and excitation-contraction coupling underlies alternans in cat heart cells. *J Physiol* **524**, 795–806.

Inesi G & de Meis L (1989). Regulation of steady state filling in sarcoplasmic reticulum. Roles of back-inhibition, leakage, and slippage of the calcium pump. *J Biol Chem* **264**, 5929–5936.

Kermode H, Chan WM, Williams AJ & Sitsapesan R (1998). Glycolytic pathway intermediates activate cardiac ryanodine receptors. *FEBS Lett* **431**, 59–62.

Klingenberg M (1989). Molecular aspects of the adenine nucleotide carrier from mitochondria. *Arch Biochem Biophys* **270**, 1–14.

Kockskämper J & Blatter LA (2002). Subcellular Ca^{2+} alternans represents a novel mechanism for the generation of arrhythmogenic Ca^{2+} waves in cat atrial myocytes. *J Physiol* **545**, 65–79.

Kodama T (1985). Thermodynamic analysis of muscle ATPase mechanisms. *Physiol Rev* **65**, 467–551.

Laughlin MR & Heineman FW (1994). The relationship between phosphorylation potential and redox state in the isolated working rabbit heart. *J Mol Cell Cardiol* **26**, 1525–1536.

Lopaschuk GD, Rebeyka IM & Allard MF (2002). Metabolic modulation. A means to mend a broken heart. *Circulation* **105**, 140–142.

Lukyanenko V & Györke S (1999). Ca^{2+} sparks and Ca^{2+} waves in saponin-permeabilized rat ventricular myocytes. *J Physiol* **521**, 575–585.

Macdonald WA & Stephenson DG (2001). Effects of ADP on sarcoplasmic reticulum function in mechanically skinned skeletal muscle fibres of the rat. *J Physiol* **532**, 499–508.

Mallet RT (2000). Pyruvate: Metabolic protector of cardiac performance. *Proc Soc Exp Biol Med* **223**, 136–148.

Mallet RT & Bünger R (1994). Energetic modulation of cardiac inotropism and sarcoplasmic reticular Ca^{2+} uptake. *Biochim Biophys Acta* **1224**, 22–32.

Mallet RT, Hartman DA & Bünger R (1990). Glucose requirement for postischemic recovery of perfused working heart. *Eur J Biochem* **188**, 481–493.

Mallet RT & Sun J (1999). Mitochondrial metabolism of pyruvate is required for its enhancement of cardiac function and energetics. *Cardiovasc Res* **42**, 149–161.

Mandel F, Kranias EG, Grassi de Gende A, Sumida M & Schwartz A (1982). The effect of pH on the transient-state kinetics of $Ca^{2+}Mg^{2+}$ATPase of cardiac sarcoplasmic reticulum. A comparison with skeletal sarcoplasmic reticulum. *Circ Res* **50**, 310–317.

Martin BJ, Valdivia HH, Bünger R, Lasley RD & Mentzer RM Jr (1998). Pyruvate augments calcium transients and cell shortening in rat ventricular myocytes. *Am J Physiol* **274**, H8–17.

Meissner G (1994). Ryanodine receptor/Ca^{2+} release channels and their regulation by endogenous effectors. *Annu Rev Physiol* **56**, 485–508.

Mellors LJ, Kotsanas G & Wendt IR (1999). Effects of pyruvate on intracellular Ca^{2+} regulation in cardiac myocytes from normal and diabetic rats. *Clin Exp Pharmacol Physiol* **26**, 889–897.

Overend CL, Eisner DA & O'Neill SC (1997). The effect of tetracaine on spontaneous Ca^{2+} release and sarcoplasmic reticulum calcium content in rat ventricular myocytes. *J Physiol* **502**, 471–579.

Philipson KD, Bersohn MM & Nishimoto AY (1982). Effects of pH on Na^{+}–Ca^{2+} exchange in canine cardiac sarcolemmal vesicles. *Circ Res* **50**, 287–293.

Poole RC & Halestrap AP (1993). Transport of lactate and other monocarboxylates across mammalian plasma membranes. *Am J Physiol* **264**, C761–782.

Ravens U & Himmel HM (1999). Drugs preventing Na^{+} and Ca^{2+} overload. *Pharmacol Res* **39**, 167–174.

Romashko DN, Marban E & O'Rourke B (1998). Subcellular metabolic transients and mitochondrial redox waves in heart cells. *Proc Natl Acad Sci U S A* **95**, 1618–1623.

Scholz TD, Laughlin MR, Balaban RS, Kupriyanov VV & Heineman FW (1995). Effect of substrate on mitochondrial NADH, cytosolic redox state, and phosphorylated compounds in isolated hearts. *Am J Physiol* **268**, H82–91.

Shannon TR & Bers DM (1997). Assessment of intra-SR free [Ca] and buffering in rat heart. *Biophys J* **73**, 1524–1531.

Smith GL & O'Neill SC (2001). A comparison of the effects of ATP and tetracaine on spontaneous Ca^{2+} release from rat permeabilised cardiac myocytes. *J Physiol* **534**, 37–47.

Vuorinen KH, Ala-Rami A, Yan Y, Ingman P & Hassinen IE (1995). Respiratory control in heart muscle during fatty acid oxidation. Energy state or substrate-level regulation by Ca^{2+}? *J Mol Cell Cardiol* **27**, 1581–1591.

Wallimann T, Wyss M, Brdiczka D, Nicolay K & Eppenberger HM (1992). Intracellular compartmentation, structure and function of creatine kinase isoenzymes in tissues with high and fluctuating energy demands: the 'phosphocreatine circuit' for cellular energy homeostasis. *Biochem J* **281**, 21–40.

Wimsatt DK, Hohl CM, Brierley GP & Altschuld RA (1990). Calcium accumulation and release by the sarcoplasmic reticulum of digitonin-lysed adult mammalian ventricular cardiomyocytes. *J Biol Chem* **265**, 14849–14857.

Xiang JZ & Kentish JC (1995). Effects of inorganic phosphate and ADP on calcium handling by the sarcoplasmic reticulum in rat skinned cardiac muscles. *Cardiovasc Res* **29**, 391–400.

Xu L, Mann G & Meissner G (1996). Regulation of cardiac Ca^{2+} release channel (ryanodine receptor) by Ca^{2+}, H^{+}, Mg^{2+}, and adenine nucleotides under normal and simulated ischemic conditions. *Circ Res* **79**, 1100–1109.

Yang Z & Steele DS (2000). Effects of cytosolic ATP on spontaneous and triggered Ca^{2+}-induced Ca^{2+} release in permeabilised rat ventricular myocytes. *J Physiol* **523**, 29–44.

Yang Z & Steele DS (2001). Effects of cytosolic ATP on Ca^{2+} sparks and SR Ca^{2+} content in permeabilized cardiac myocytes. *Circ Res* **89**, 526–533.

Yanos J, Patti MJ & Stanko RT (1994). Hemodynamic effects of intravenous pyruvate in the intact, anesthetized dog. *Crit Care Med* **22**, 844–850.

Zhou Z, Lasley RD, Hegge JO, Bünger R & Mentzer RM Jr (1995). Myocardial stunning: a therapeutic conundrum. *J Thorac Cardiovasc Surg* **110**, 1391–1400.

Zima AV, Kockskämper J & Blatter LA (2002). Pyruvate-mediated effects on cardiac Ca^{2+} signaling. *Biophys J* **82**, 71a.

Zweier JL & Jacobus WE (1987). Substrate-induced alterations of high energy phosphate metabolism and contractile function in the perfused heart. *J Biol Chem* **262**, 8015–8021.

Acknowledgements

The authors are thankful to Dr L. Maier for insightful discussions and comments on the manuscript. We would like to thank Dr D. M. Bers and his staff for cell preparation, and Dr Claudia G. Perez for sharing her expertise with the single channel experiments. Cariporide was a generous gift from Aventis Pharma Deutschland GmbH. This work was supported by the NIH (NIH R01HL62231 to L.A.B. and NIH R01HL62571 to R.M.A.) and the AHA (AHA Grant-in Aid 9950382N to R.M.A.). J.K. was a recipient of fellowships from the Falk Foundation (Loyola University Chicago) and the Deutsche Forschungsgemeinschaft (DFG).

Author's present address

J. Kockskämper: Abteilung Kardiologie und Pneumologie, Georg-August-Universität, Robert-Koch-Strasse 40, 37075 Göttingen, Germany.